Journal of Medicinal Chemistry

Article

A Novel Class of Oral Direct Renin Inhibitors: Highly Potent 3,5-Disubstituted Piperidines bearing a Tricyclic P3–P1 Pharmacophore

Nils Ostermann, Simon Ruedisser, Claus Ehrhardt, Werner Breitenstein, Andreas L. Marzinzik, Edgar Jacoby, Eric Vangrevelinghe, Johannes Ottl, Martin Klumpp, Constanze Hartwieg, Frederic Cumin, Ulrich Hassiepen, Jörg Trappe, Richard C Sedrani, Sabine Geisse, Bernd Gerhartz, Paul Richert, Eric Francotte, Trixie Wagner, Markus Krömer, Takatoshi Kosaka, Randy L Webb, Dean F Rigel, Juergen Klaus Maibaum, and Daniel K Baeschlin

J. Med. Chem., **Just Accepted Manuscript** • DOI: 10.1021/jm301706j • Publication Date (Web): 29 Jan 2013

Journal of Medicinal Chemistry is published by the American Chemical Society. 1155 Sixteenth Street N.W., Washington, DC 20036

	Institutes for BioMedical Research Webb, Randy; Novartis Pharmaceuticals Corp., Novartis Institutes for BioMedical Research Rigel, Dean; Novartis Pharmaceuticals Corp., Novartis Institutes for BioMedical Research Maibaum, Juergen; Novartis Pharma AG, Novartis Institutes for BioMedical Research Baeschlin, Daniel; Novartis Pharma AG, Novartis Institutes for BioMedical Research

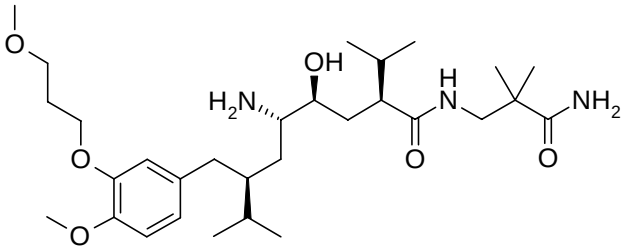

Aliskiren (**1**): IC_{50} (plasma renin) = 0.6 nM

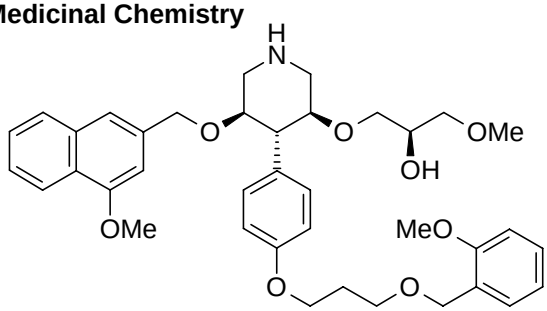

2: IC_{50} (plasma renin) = 8.9 nM

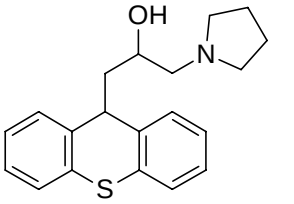

(*rac*)-**3**

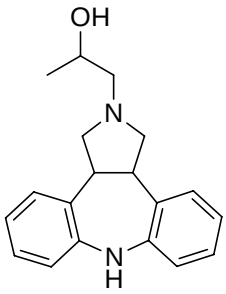

(*rac*)-**4**

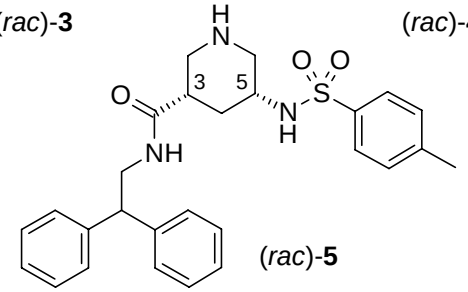

(*rac*)-**5**

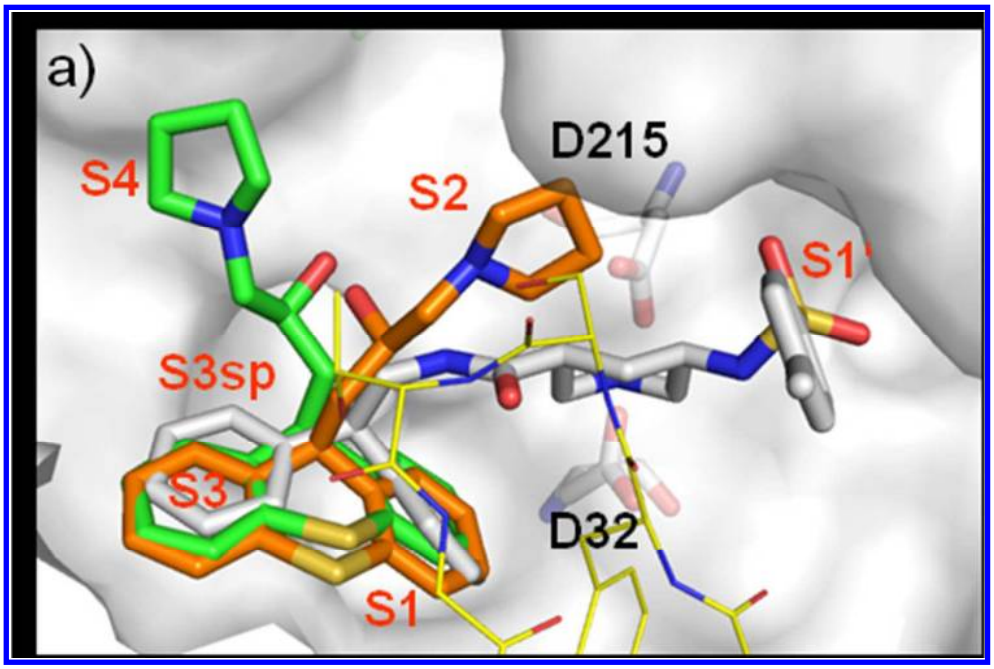

82x54mm (150 x 150 DPI)

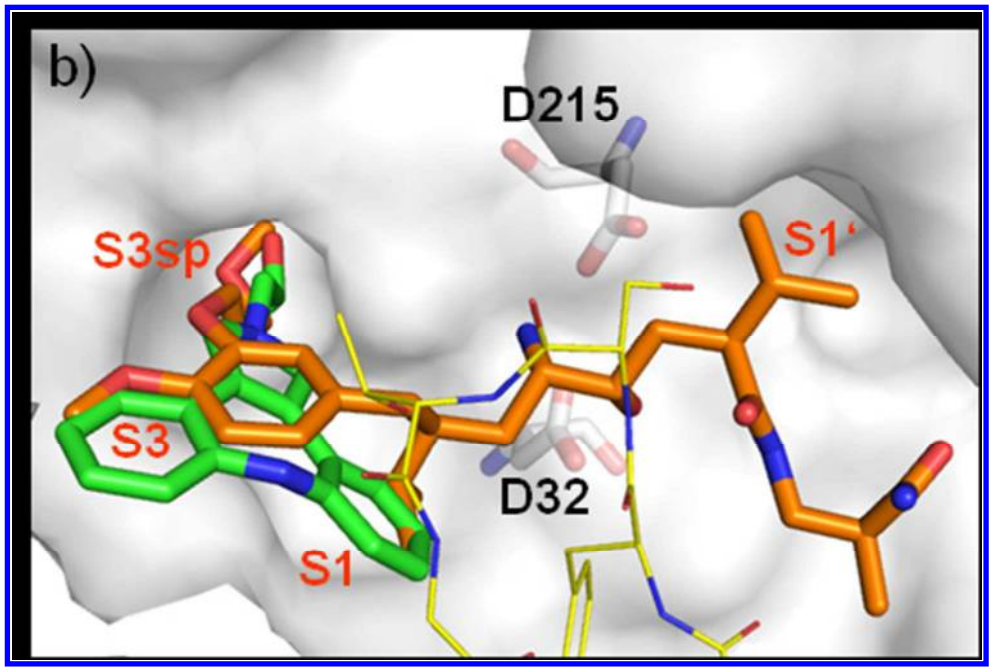

81x54mm (150 x 150 DPI)

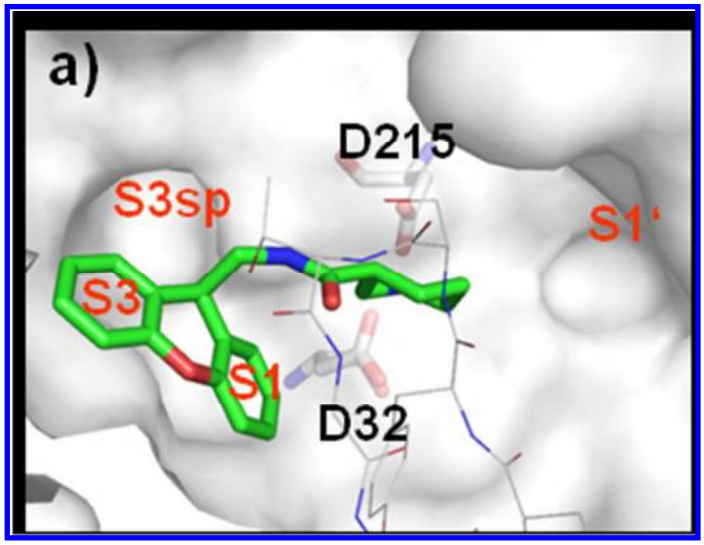

57x44mm (150 x 150 DPI)

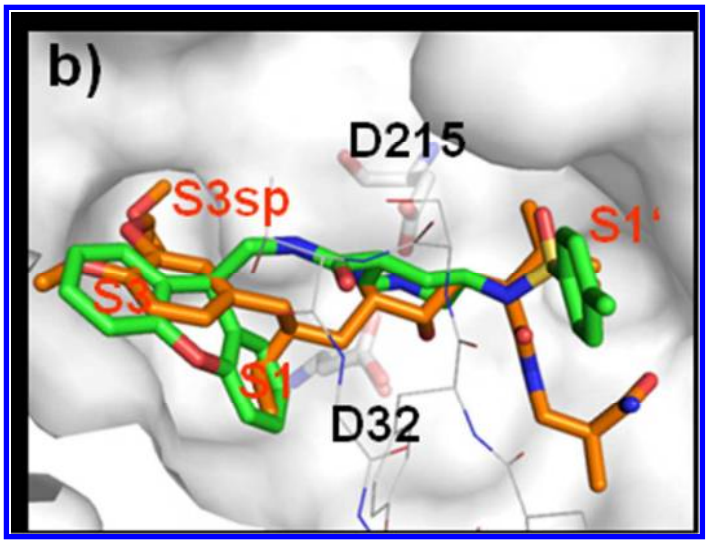

58x44mm (150 x 150 DPI)

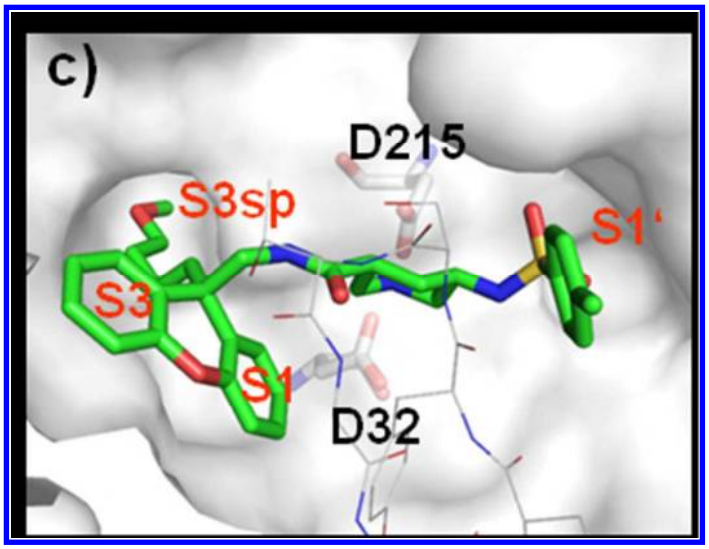

58x44mm (150 x 150 DPI)

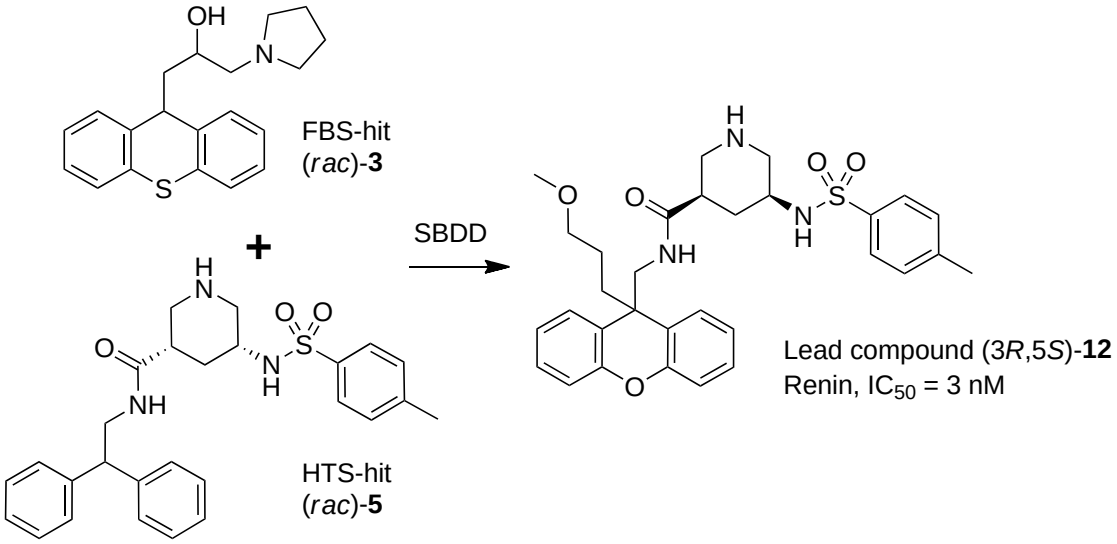
OH
N
S
FBS-hit
(rac)-3
+
H
N
O
O
S
N
H
O
NH
HTS-hit
(rac)-5
SBDD
H
N
O
O
S
O
N
H
O
NH
O
Lead compound (3R,5S)-12
Renin, IC50 = 3 nM

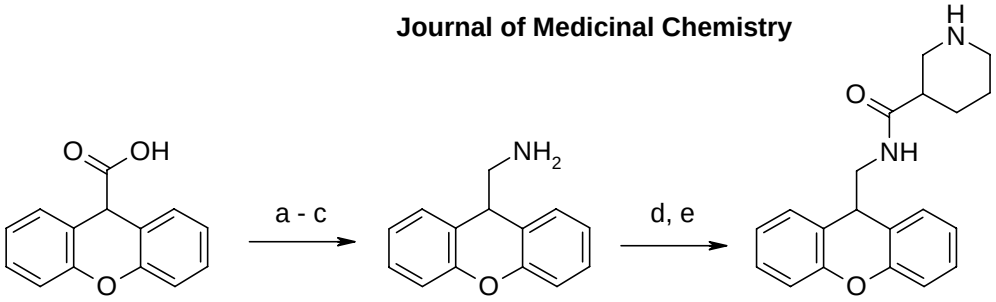

7 **8** *(rac)*-**6**

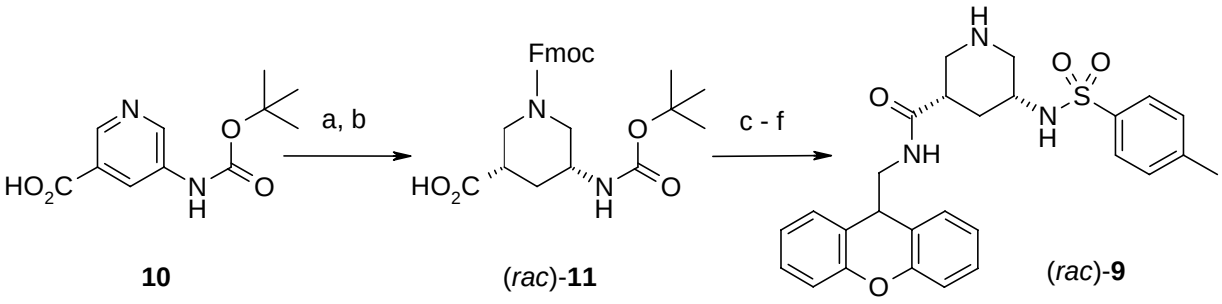

10 (*rac*)-**11** (*rac*)-**9**

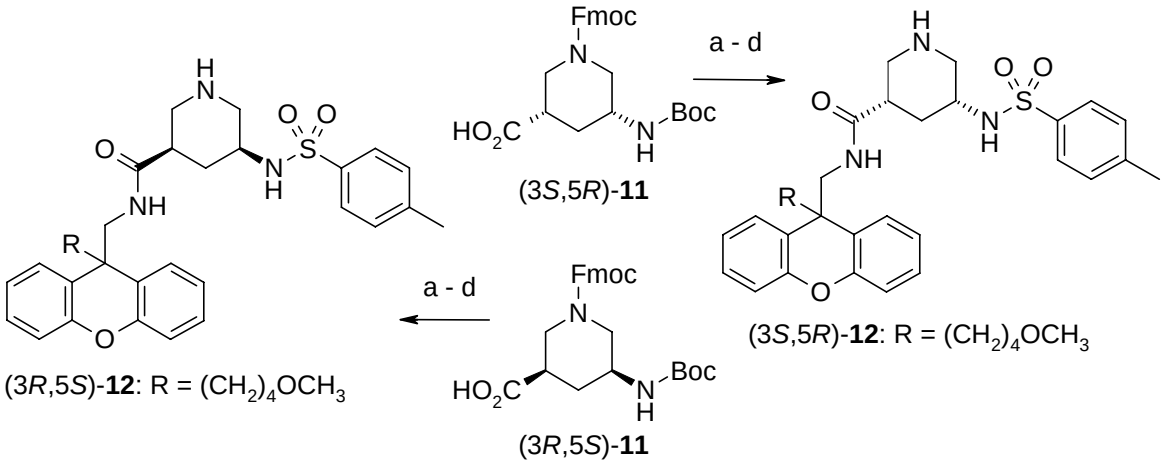
Fmoc
N
HO2C
N
Boc
H
(3S,5R)-11
a - d
H
N
O
O
S
O
N
H
NH
R
O
(3S,5R)-12: R = (CH2)4OCH3
a - d
Fmoc
N
HO2C
N
Boc
H
(3R,5S)-11
H
N
O
O
S
O
N
H
NH
R
O
(3R,5S)-12: R = (CH2)4OCH3

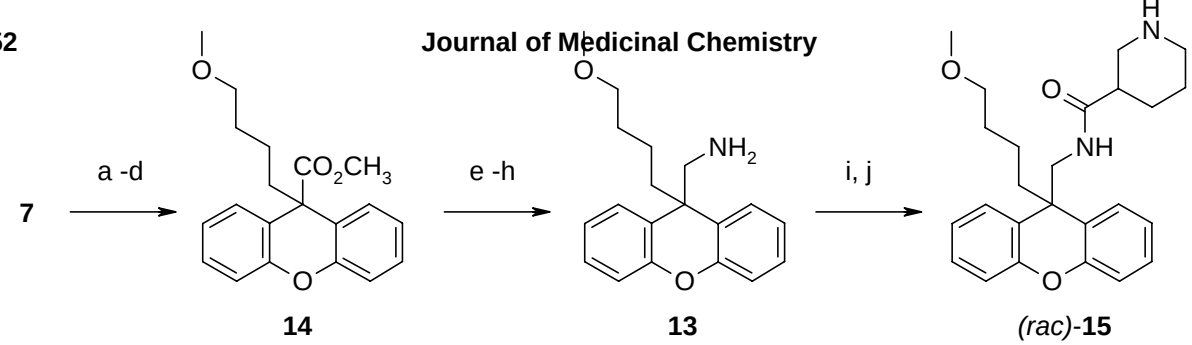
7
a -d
CO2CH3
e -h
NH2
i, j
NH
O
14
13
(rac)-15

A Novel Class of Oral Direct Renin Inhibitors: Highly Potent 3,5-Disubstituted Piperidines bearing a Tricyclic P_3–P_1 Pharmacophore

Nils Ostermann,[a] Simon Ruedisser,[a] Claus Ehrhardt,[a] Werner Breitenstein,[a] Andreas Marzinzik,[a] Edgar Jacoby,[a] Eric Vangrevelinghe,[a] Johannes Ottl,[a] Martin Klumpp,[a] J. Constanze D. Hartwieg,[a] Frederic Cumin,[a] Ulrich Hassiepen,[a] Jörg Trappe,[a] Richard Sedrani,[a] Sabine Geisse,[a] Bernd Gerhartz,[a] Paul Richert,[a] Eric Francotte,[a] Trixie Wagner,[a] Markus Krömer,[a] Takatoshi Kosaka,[b] Randy L. Webb,[c] Dean F. Rigel,[c] Jürgen Maibaum,[a] and Daniel K. Baeschlin[a]*

[a] Novartis Pharma AG, Institutes for BioMedical Research, Novartis Campus, CH-4056 Basel, Switzerland, [b] Novartis Institutes for BioMedical Research, Horsham, West Sussex RH12 5AB, UK. [c] Novartis Pharmaceuticals Corp., Novartis Institutes for BioMedical Research, East Hanover, New Jersey

KEYWORDS. Renin inhibitor, fragment based screening, 3,5-disubstituted piperidines

ABSTRACT. A small library of fragments comprising putative recognition motifs for the catalytic dyad of aspartic proteases was generated by in silico similarity searches within the corporate compound deck based on rh-renin active site docking and scoring filters. Subsequent screening by NMR identified the low-affinity hits **3** and **4** as competitive active site binders,

which could be shown by X-ray crystallography to bind to the hydrophobic S_3-S_1 pocket of rh-renin. As part of a parallel multiple hit–finding approach, the 3,5-disubstituted piperidine (*rac*)**-5** was discovered by HTS using a enzymatic assay. X-ray crystallography demonstrated the eutomer (*3S,5R*)**-5** to be a peptidomimetic inhibitor binding to a nonsubstrate topography of the rh-renin prime site. The design of the potent and selective (*3S,5R*)**-12** bearing a P_3^{sp}-tethered tricyclic P_3–P_1 pharmacophore derived from **3** is described. (*3S,5R*)**-12** showed oral bioavailability in rats and demonstrated blood pressure lowering activity in the double-transgenic rat model.

Hypertension, the chronic elevation of systemic blood pressure, is a major health risk in the Western world with approximately 29% of the adult population worldwide projected to develop this condition by 2025.[1] High blood pressure increases the risk of stroke, heart disease, and kidney failure causing approximately 277,000 deaths in the US in 2002 alone.[2] In a majority of hypertension patients, blood pressure is still controlled inadequately or not at all despite the existence of a variety of drug treatments and as a consequence, a high unmet medical need for more efficient drug therapy remains. The renin–angiotensin–aldosterone system (RAAS) plays a central role in the regulation of blood pressure as revealed by multiple preclinical and clinical studies employing angiotensin converting enzyme (ACE) inhibitors, angiotensin receptor (AT) antagonists and direct renin inhibitors (DRIs).[3] The first step in this regulatory cascade is the cleavage of angiotensinogen as the only known substrate for the aspartic protease renin to generate the decapeptide angiotensin I. Subsequent cleavage by ACE produces the octapeptide angiotensin II, which is the principal mediator of RAAS and which exerts its major effects through the AT_1 and AT_2 receptors. Blockade of the RAAS at its source by direct inhibition of the first and rate-limiting step involving renin, has been recognized for many years as an

attractive approach to treat hypertension.[4] Hence, DRIs have been considered to provide potential clinical benefits over other antihypertensive drugs interfering with the RAAS, such as ACEi and AT_1 receptor antagonists.[5] Major efforts and substantial progress made in the design of potent and selective non-peptide DRIs have culminated in the discovery of the first-in-class orally active **1** (aliskiren, Rasilez, Tekturna; Figure 1) now approved for the once daily treatment for hypertension.[6-8]

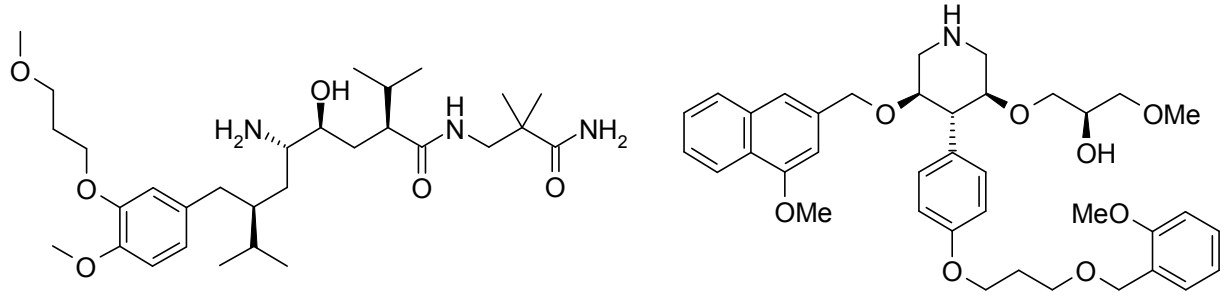

Aliskiren (**1**): IC_{50} (plasma renin) = 0.6 nM

2: IC_{50} (plasma renin) = 8.9 nM

Figure 1. Potent non-peptide direct renin inhibitors.

Several diverse classes of non-peptide DRIs have evolved through recent years, as the topographical space of the renin active site targetable for inhibitor design has significantly expanded.[8,9] The hydroxyethylene dipeptide isostere analogue **1**, designed based on a S_3–S_1 topological concept, emulates the extended β-strand binding active site conformation of renin and, in addition, tightly interacts with the nonsubstrate S_3^{sp} pocket.[10] The class of 3,4-disubstituted piperidine GRAB peptidomimetics[11] (cf. **2**, Figure 1), first reported in 1999, bind to a fundamentally distinct active site topography characterized by a newly formed hydrophobic pocket resulting from major concerted movements of the β-hairpin loop to an "open flap" ligand-binding conformation.[12] The center piperidine interacts as a basic transition-state surrogate with the catalytic Asp_{32} and Asp_{215} by forming favorable charge-enforced H-bonds. A second

generation GRAB peptidomimetic bearing a 3,9-diazabicyclo[3.3.1]nonene center scaffold has undergone clinical trials.[13] Furthermore, the 2,4-diaminopyrimidine and most recently the alkylamine class of DRIs have attracted attention.[8,9,14] Our continued interest in the discovery of a "best-in-class" DRI prompted a broad screening program toward new druglike leads by applying multiple approaches in parallel. These included high-throughput screening (HTS) using an enzymatic and a competitive ligand binding assay, a combined NMR/X-ray fragment-based screen of focused libraries, as well as in silico 3D pharmacophore searches. These integrated efforts turned out to be remarkably complementary in identifying attractive diverse chemotype hits from different sources.[15] We report herein the discovery of 3,5-disubstituted piperidines bearing a tricyclic P3–P1 unit as a novel and potent direct renin inhibitor class through the combination of structural features of a HTS hit and a fragment binding weakly to renin identified by a NMR/X-ray fragment based screen.

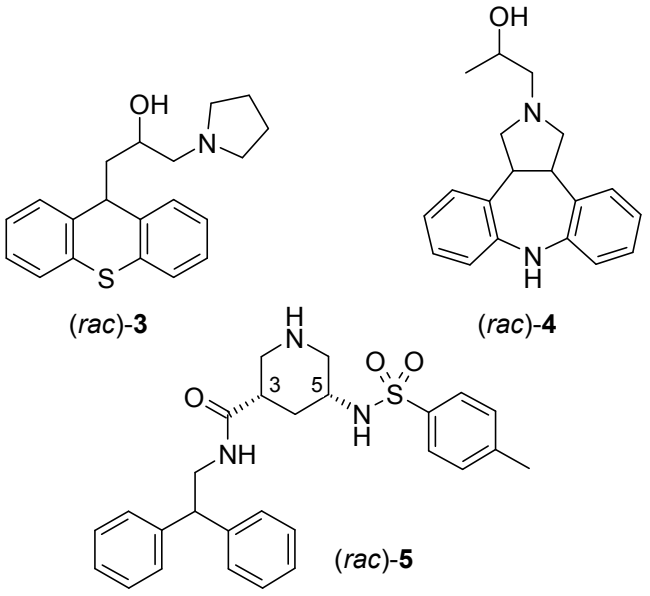

Figure 2. Fragment-based screening hits *(rac)*-**3** and *(trans,rac)*-**4,** and HTS hit (*rac*)-**5**.

We designed a small fragment screening library intended to target specifically the family of aspartic proteases and comprising "privileged" recognition motifs related to transition-state mimetics, such as amino alcohols, as well as basic 5- and 6-membered cycloalkylamine transition-state (TS) surrogates inspired by the structures of known aspartic protease inhibitors.[16] 2D and 3D in silico database mining tools were applied for substructure and similarity searches within the Novartis deck of physically available compounds. To further reduce the fragment library to a size compatible with NMR screening capacity, docking and scoring using GOLD[17] and subsequent rescoring analyses by Cscore[18] were performed. A total of 113 compounds were finally selected and initially screened by NMR for binding to rh-renin, using ligand observation techniques such as T1ρ relaxation experiments. Several members of the biased fragment library, including *(rac)*-**3** and *(trans,rac)*-**4** (Figure 2; NMR K_d >500 μM; IC_{50} >100 μM in the FRET biochemical assay), were found to have very weak binding affinities to rh-renin and, in addition, to be active site ligands as determined by NMR competition experiments in the presence of **1**.[19]

Cocrystallization as well as soaking experiments using different crystal forms of recombinant human (rh) apo-renin,[19] were subsequently performed for more than twenty fragment hits validated by NMR as low-affinity binders. We were very gratified that crystal structures of two of these fragments, i.e., the competitive active site binders *(rac)*-**3** and *(trans,rac)*-**4**, in complex with rh-renin could be solved thereby elucidating their unexpected binding mode to the nonprime active site of the enzyme (Figure 3). Both the hydrophobic 9*H*-thioxanthene moiety of **3** and the 5*H*-dibenzoazepine scaffold of **4** were found to be in close van der Waals contact and to completely fill the open contiguous hydrophobic S_3–S_1 binding site of human renin with the flap β-hairpin (residues Tyr_{75}, Ser_{76}, Thr_{77} and Gly_{78}) in a closed conformation. The adopted bent "butterfly" conformations of the heteroaryl portions of **3** and **4** allow to bridge both hydrophobic

phenyl moieties accommodating a position considerably deeper inside the S_3 and S_1 pockets, respectively, compared to the P_3 and P_1 binding motifs of known peptide peptidomimetic renin inhibitors as well as the topological transition-state mimetic **1** (Figure 3b).[10] As a consequence of the binding poses of the tricylic scaffolds of **3** and **4** within the S_3–S_1 cavity, both the hydroxylated side chains and the nitrogen atoms of the pyrrolidine moieties of the ligands were in remote positions relative to the Asp_{32} and Asp_{215} carboxylates. The amino alcohol side chain of **3**, adopting an axial conformation in the crystal structure obtained by using the racemate for soaking, exhibited different binding orientations for the two rh-renin molecules in the asymmetric unit of the crystal which have been fitted with the R- and S-enantiomers and were located in large distance from the enzyme catalytic dyad (Figure 3a). This was surprising to us in view of the target-biased fragment library design based on the query for privileged transition-state surrogate motifs for aspartic proteases. The observed binding mode suggests to us that the binding of **3** and **4** is mainly entropy–driven by hydrophobic interactions to the hydrophobic S_3–S_1 cavity of renin. This specific binding site is now well recognized as a "hydrophobic hot spot" and a key topography to target for the design of potent direct renin inhibitors.[8-13]

Most strikingly, the 2-hydroxypropyl side chain of **4** extended into the nonsubstrate S_3^{sp} cavity by extruding the ordered water of apo-renin and forming a H-bond to the carbonyl of Thr_{216} located close to the bottom of this distinct rigid channel (Figure 3b). To our knowledge, a H-bonding opportunity involving Thr_{216} has not been observed previously for other chemotype renin inhibitors.[8] It should be noted that *(trans,rac)*-**4** was build with the (*R*)-configuration of the hydroxyl group. A fit with the (S)-configuration of the hydroxyl group would be possible and would result in an H-bond between the hydroxyl group of **4** and the NH of the Tyr_{14} backbone. As a result, fragment screening by NMR and X-ray has allowed two key design principles to be

"rediscovered", i.e., targeting of the S_1–S_3 hydrophobic hot spot and exploitation of the S_3^{sp} binding site of human renin: both principles have been critical for the conception of the topological transition-state mimetic inhibitor **1**,[10b] and have been subsequently applied to the design of other non-peptide classes of DRIs.[8-13] In general, this work represents an impressive illustration of the power of biophysical screening approaches for active site mapping by low-affinity ligands of renin as a member of the aspartic protease family.

In particular **3** gained our attention as an attractive scaffold for further optimization by a fragment growing approach. We sought to expand the heteroaryl scaffold by targeting binding interactions to the catalytic Asp_{32} and/or Asp_{215} as well as the prime site specificity pockets of human renin in the quest to substantially gain binding affinity by several orders of magnitude. In the course of our initial exploratory work on the structure–activity relationship (SAR) for **3**, a high-throughput biochemical screen of the Novartis compound deck using a miniaturized fluorescence–polarization assay identified the racemic *cis*-configured 3,5-disubstituted piperidine **5** (IC_{50} of 1.2 μM, Figure 2, Table 1) as a novel chemotype renin inhibitor. *(Rac)*-**5** originated from a split–and–mix library comprising some 950 compounds which had been specifically designed to target aspartic proteases.[20] The general library concept had been based on the hypothesis that the positively charged nitrogen of the piperidine "privileged" scaffold[8,12] could interact with the enzyme catalytic dyad, and that the NH of the (sulfon)amide residues are potentially involved in H-bonds with backbone atoms of the flap region. The crystal structure of rh-renin in complex with *(rac)*-**5** indicated that only the (3*S*,5*R*)-enantiomer was bound in the active site (Figure 3a).[21] The basic 3,5-disubstituted center piperidine was indeed confirmed to function as a transition-state surrogate with the nitrogen atom being placed symmetrically between Asp_{32} and Asp_{215} to form a charge–charge interaction. Inhibitor (3*S*,5*R*)-**5** emulates the

extended substrate β-strand binding topography of the renin active site by spanning the nonprime S_3–S_1 recognition sites and the prime region with the flap β-hairpin in a closed conformation. This is in contrast to the class of 3,4-disubstituted piperidine GRAB peptidomimetics, such as **2**, binding to a very distinct "open flap" topography of human renin.[12] The carboxamide at the piperidine C3 of **5** forms H-bonds to Gly_{217} and Ser_{76} of the flap β-hairpin, whereas the sulfonamide group is involved in two water–mediated H-bonds with the NH in close distance to the flap Arg_{74} and one sulfonyl oxygen atom interacting with Gly_{34} of the prime site. The diphenylmethane pharmacophore of (3*S*,5*R*)-**5** resides in the large S_1–S_3 cavity in a very similar fashion as observed for *(rac)*-**3** and *(rac)*-**4** (Figure 3).

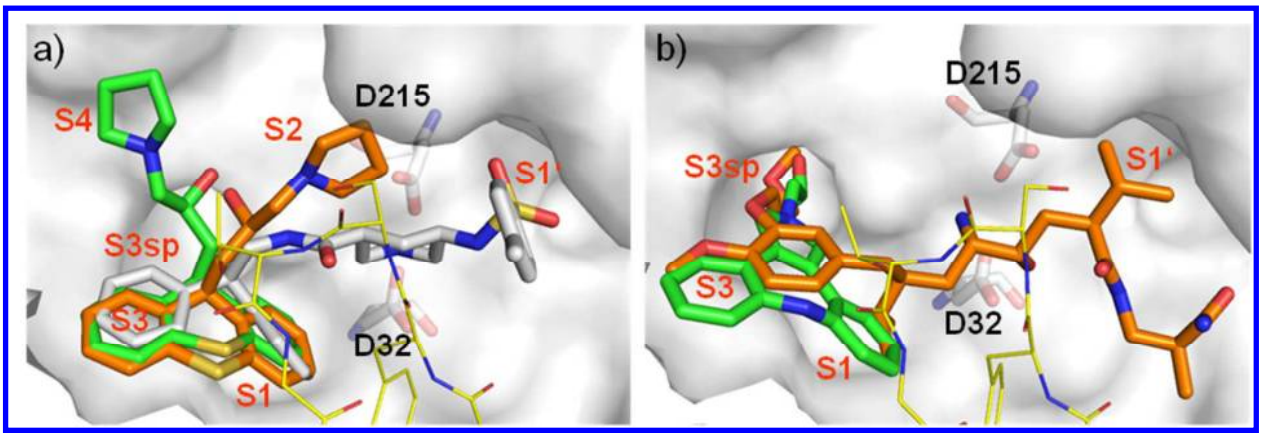

Figure 3. (a) Crystal structures of the (*S*)-configured 9*H*-thioxanthene **3** (shown as stick model in green color) and (*R*)-**3** (orange color), both superimposed with the 3,5-piperidine inhibitor (3*S*,5*R*)-**5**[19] (grayish color) bound to rh-renin. Shown is the solvent accessible surface of the active site of renin. Residues of the flap β-hairpin (residues Tyr_{75}, Ser_{76}, Thr_{77} and Gly_{78}) in a closed conformation are depicted for the complex of renin with (3*S*,5*R*)-**5** in yellow as thin lines and have been omitted from the protein surface calculation. The oxygen and nitrogen atoms of the ligands are colored in red and blue, respectively. (b) Superposition of the crystal structure of

the 5*H*-dibenzazepine **4** (shown as stick model in green color) and the topological transition-state mimetic **1** (orange color; PDB code 2v0z) in complex with rh-renin. The crystal structure obtained with *(trans,rac)*-**4** was build with the (*R*)-configuration of the hydroxyl group in **4** (as shown). Residues of the flap β-hairpin (residues Tyr_{75}, Ser_{76}, Thr_{77} and Gly_{78}) in a closed conformation are depicted for the complex of rh-renin with **4** in yellow as thin lines and have been omitted from the protein surface calculation.

A particularly intriguing feature of this new class of topological peptidomimetic inhibitors is the unprecedented binding mode to the prime site of rh-renin. First, the sulfonamide oxygens of **5** were found to bind into the S_1' pocket, which is considered to preferentially accommodate hydrophobic residues.[22] Superposition with the X-ray structure of **1**[10] revealed a close overlap of both sulfonyl oxygens with the S_1' isopropyl group of the hydroxyethylene dipeptide isostere (cf. Figure 4b for **9**). The dual character of weakly polar sulfonyl groups as a H-bond acceptor and as a hydrophobic group capable to form van der Waals contacts with nonpolar atoms in a hydrophobic environment has been discussed recently for ligand–protein interactions.[23] Secondly, the geometry of the sulfonamide spacer positions the tolyl residue between the proline-rich loop (Met_{289}–Thr_{298}) and the flap region (Thr_{72}–Ser_{81}), thereby leaving the S_2' site unoccupied. This nonsubstrate binding topography at the prime site of the renin catalytic cleft, which further extends toward solvent space, is primarily the result of a slight conformational movement of the proline loop, which has not been recognized previously to the best of our knowledge.

The X-ray structural information gained for the polycyclic heteroaryl ligands **3** and **4** and the piperidine (3*S*,5*R*)-**5** suggested to us several avenues for further optimization by merging key structural features. The rigid tricyclic framework tightly binding into the hydrophobic S_3–S_1

cavity was considered to offer some advantage over the more flexible diphenylmethane moiety. More importantly, the X-ray data provided reasonable evidence for the three–atom carboxamide linker of **5** to be also suitable to connect the tricyclic portion of **3** to a TS surrogate targeting the catalytic dyad of the enzyme active site. In order to probe the concept, the readily accessible 9*H*-xanthene derivative *(rac)*-**6** replacing the 9*H*-thioxanthene heterocycle of *(rac)*-**1** was initially synthesized (Scheme 1). In brief, the commercial carboxylic acid **7** was transformed in 3 steps to the primary amine **8**, followed by PyBOP–mediated coupling to *(rac)*-1-Boc-piperidine-3-carboxylic acid and final N-debocylation to afford *(rac)*-**6** in 13% yield. Compound **6** was found to be completely inactive toward rh-renin in the FRET biochemical assay at the highest concentration tested (100 μM; Table 1). However, we were much intrigued by the fact that the crystal structure of **6** in complex with rh-renin could be solved (Figure 4a), despite the very low apparent binding affinity of the ligand. As was expected by modeling, the observed binding mode of **6** was very similar to the interactions of the corresponding substructures of rh-renin–bound (3*S*,5*R*)-**5**. The tricyclic scaffolds of both ligands accommodated by the S_3–S_1 cavity closely overlapped, apart from minor geometrical differences due to the nature of the ring heteroatoms, as was the case for the center piperidines with the basic nitrogen atoms in the pivotal position between the catalytic aspartates. Also, the geometry and lengths of the H-bonds exerted by the carboxamide spacer of **6** to Gly_{217} and Ser_{76} of the flap β-hairpin were comparable to those observed for **5**. The X-ray data demonstrated to us that it is indeed possible to grow from the S_3–S_1 fragment toward the catalytic Asp_{32} and Asp_{215} by the proper choice of a linear spacer group and connecting to a transition-state analog, albeit this had not resulted in a significant improvement in the in vitro potency for **6**.

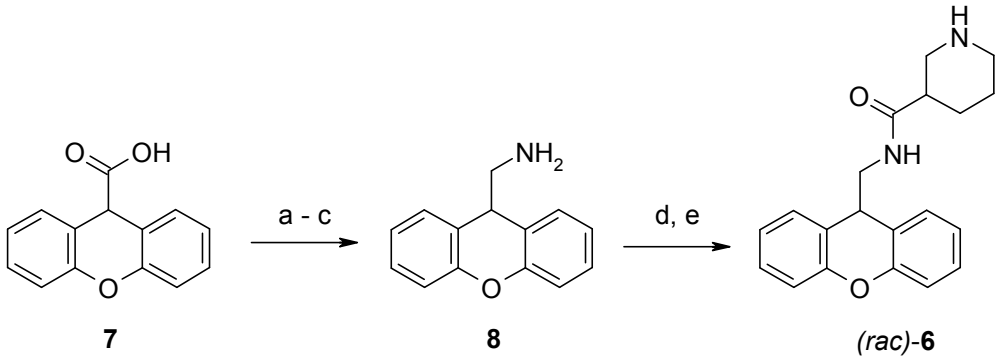

Scheme 1. Synthesis of *(rac)*-**6**: (a) EEDQ, benzylamine, CH_2Cl_2, RT, 40%; (b) $LiAlH_4$, $AlCl_3$, THF, 0°C to 50°C, 72%; (c) H_2, 10% Pd/C, EtOH, RT, 99%; (d) 1-*Boc*-piperidine-3-carboxylic acid, PyBOP, Et_3N, CH_3CN, RT, 79%; (e) 4 M HCl–dioxane, RT, 56%.

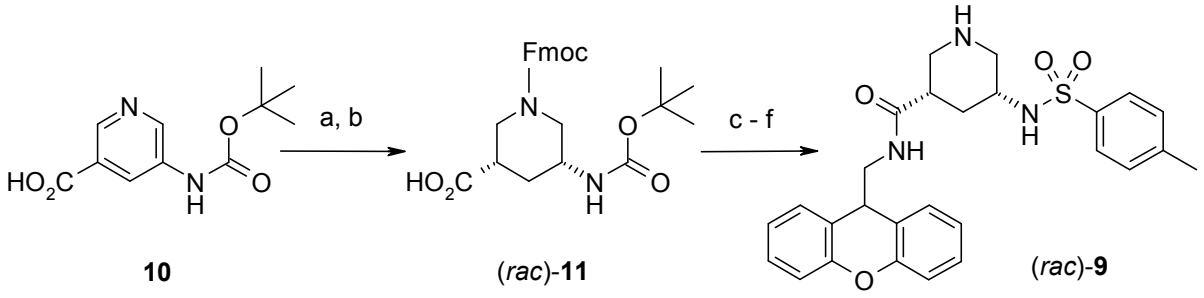

Scheme 2. Synthesis of *(rac)*-**9**: (a) Nishimura catalyst, 25% aq. NH_4OH–H_2O, RT, 24 h , 40%; (b) Fmoc-succinimide, THF–H_2O 1:1, $NaHCO_3$, 88%; (c) 4M HCl–dioxane, RT, 96%; (d) toluene-4-sulfonyl chloride, aq. K_2CO_3, dioxane, 0°C, 54%; (e) **8**, HCTU, DIPEA, CH_2Cl_2–CH_3CN 1:1, 0°C; (f) CH_2Cl_2–piperidine 4:1, RT, 5% (two steps).

Next, we envisaged the introduction of the sulfonamide side chain to the piperidine C3 of *(rac)*-**6** as suggested by the structural overlay of renin–bound **5** and **6** (overlay not shown). Accordingly, *(rac)*-**9** was prepared starting from commercial 5-Boc-amino-nicotinic acid **10** (Scheme 2) via

hydrogenation, subsequent *N*-Fmoc protection and precipitation from water to provide the versatile building block (*rac*,*cis*)-**11** in 35% yield. *N*-Boc deprotection followed by sulfonamide formation and coupling with amine **8** afforded Fmoc protected **9**. The amide coupling reaction and the final Fmoc deprotection step proceeded to give *(rac)*-**9**, although in only 5% overall yield. Notably, (*rac*)-**9** demonstrated to be a potent inhibitor of rh-renin (IC_{50} of 0.09 μM) in the FRET assay (Table 1).

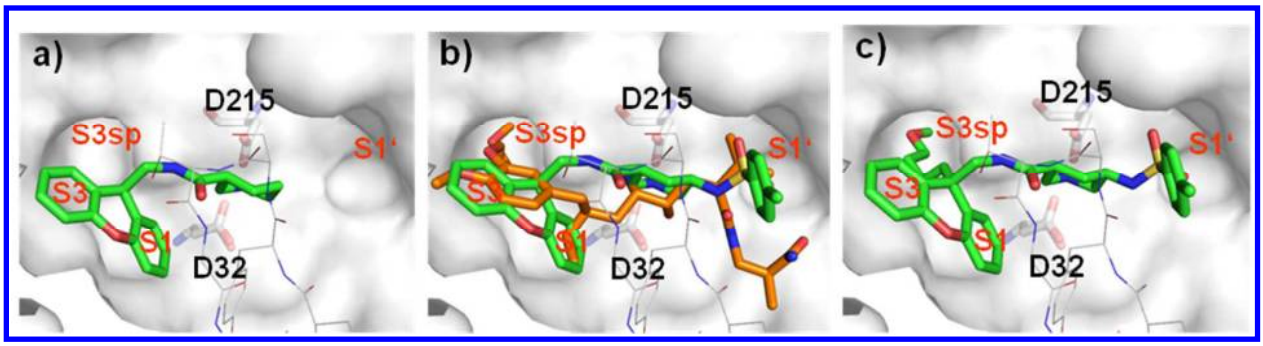

Figure 4. Crystal structures of rh-renin in complex with (a) compound **6** (shown as stick model in green color); (b) inhibitor **9** (stick model in green color) superimposed with **1** (orange color; PDB code 2v0z); (c) compound **12** (as stick model in green). Shown is the solvent accessible surface of the active site of rh-renin. Residues of the flap β-hairpin are only depicted for the rh-renin–**9** complex in grayish as thin lines and have been omitted for protein surface calculation. The catalytic aspartates are shown as stick model. Oxygen, nitrogen and sulfur atoms are shown in red, blue and yellow color, respectively. The ligand electron density of crystal structures obtained with *(rac)*-**6, 9 and 12** was better compatible with the piperidine ring in the 3S, 5R configuration and was therefore build as 3S for **6** and 3S, 5R for **9** and **12**.

The crystal structure obtained by soaking of (rac)-**9** into rh-renin crystals confirmed the expected binding pose (Figure 4b) and revealed a perfect overlap with the tricyclic scaffold of **6** on one

hand, by filling the S_3–S_1 cavity (Figure 4a), as well as with the tolylsulfonamide portion of (3*S*,5*R*)-**5**, interacting to the prime site (Figure 3a). Also, both phenyl residues of the diphenylmethyl moiety of renin–bound (3*S*,5*R*)-**5** were in almost identical positions when compared to the tricycle of (rac)-**9**, with only a very minor difference in the planar orientations observed for the respective P_1 phenyl groups. The 13-fold potency increase for (*rac*)-**9** suggested the conformationally rigid P_1–P_3 scaffold to be superior as compared to the more flexible diphenylmethyl pharmacophore.

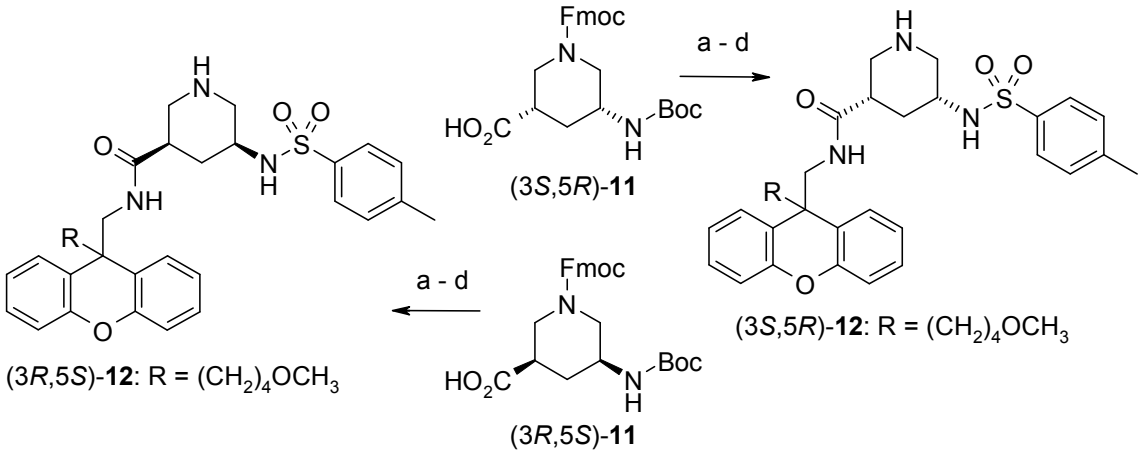

Scheme 3. Synthesis of (3*S*,5*R*)-**12** and (3*R*,5*S*)-**12**: (a) **13**, HCTU, DIPEA, CH_2Cl_2–CH_3CN 1:1, RT, 42%; (b) 0.4 M HCl–dioxane, RT, 68%; (c) toluene-4-sulfonyl chloride, DMAP, pyridine; (d) CH_2Cl_2–piperidine 4:1, RT, 39% (two steps).

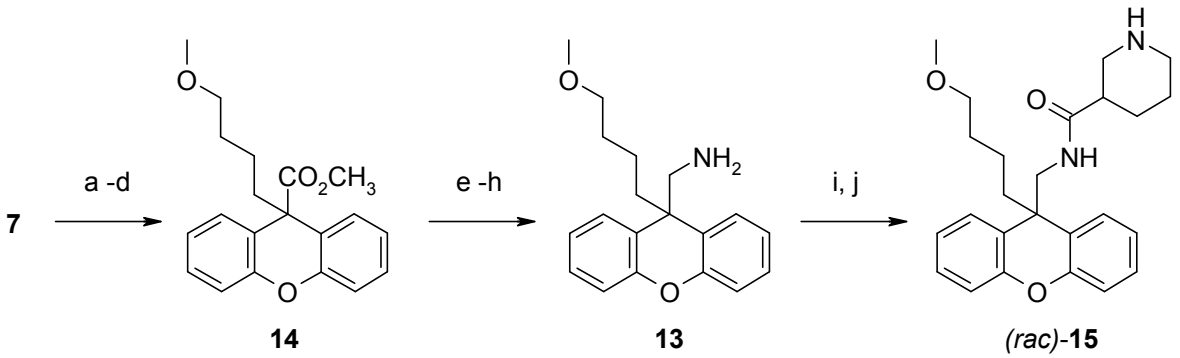

Scheme 4. Synthesis of *(rac)*-**15**: (a) Cs_2CO_3, CH_3I, DMF, RT, 97%; (b) LDA, 4-bromo-1-butene, HMPA, THF, –78°C to 0°C, 81%; (c) 9-BBN, THF, 40°C; then H_2O_2, 2 M NaOH, 63%; (d) MeI, NaH, DMF, 0°C to RT, 90%; (e) 2 M NaOH, dioxane, 60°C; (f) PyBOP, benzylamine, Et_3N, DMF, 0° to RT, 83% (two steps); (g) $BH_3 \cdot Me_2S$, THF, 150°C, microwave, 86%; (h) 10% Pd/C, EtOH, RT, 78%; (i) 1-*Boc*-piperidine-3-carboxylic acid, HCTU, Et_3N, 0°C to RT, 87%; (j) 4 M HCl–dioxane, RT, 84%.

Most notably, the X-ray structure of the rh-renin–inhibitor **9** complex revealed the unsubstituted equatorial C9 position of the tricyclic portion to be located at the entrance of the nonsubstrate S_3^{sp} pocket, thereby providing an attractive trajectory for flexible P_3^{sp} side chain extensions toward this important binding site. Inspection of the superimposed crystal structure of rh-renin bound inhibitor **1** (Figure 4b) and molecular modeling suggested a methoxybutyl chain attached to the central ring to be optimal in length in order to fill the cavity and to potentially induce a H-bond interaction to Tyr_{14} by the terminal methoxy group similarly to **1**. Other options for introducing a suitable P_3^{sp} substituent, for example at the P_3 phenyl of the tricycle, appeared to be plausible as well, but were not considered at this stage due to the expected higher synthetic complexity.

In order to probe the design concept, the target compound **12** was initially prepared as the racemate from readily available (*rac*)-**11** and amine **13** (Schemes 3 and 4). Side chain alkylation of the methyl ester of **7** via deprotonation using LDA and reaction with 4-bromo-1-butene was followed by 9-BBN–mediated hydroboration and O–methylation to afford intermediate **14** in 45% yield (Scheme 4). Transformation of **14** to the amine **13** was accomplished in overall 4 steps (56% yield) via reduction of the corresponding benzylamide intermediate with borane-dimethylsulfide under microwave conditions and hydrogenolysis of the resulting benzylamine derivative. A reversed reaction sequence by first starting with HCTU coupling of **13** to (*rac*)-**11** (42% yield), followed by *N*-debocylation, sulfonylation and Fmoc deprotection was found to be more advantageous and afforded (*rac*)-**12** in acceptable overall yield. (*Rac*)-**12** inhibited rh-renin with an IC_{50} of 0.004 μM, and hence was >20-fold more potent in vitro as compared to (*rac*)-**9** lacking the methoxybutyl side chain at the tricyclic P_3–P_1 scaffold (Table 1). This prompted us to prepare the pure enantiomers (3*S*,5*R*)-**12** and (3*R*,5*S*)-**12** from (3*S*,5*R*)-**11** and (3*R*,5*S*)-**11** (Scheme 3), respectively, which were accessible from racemate **11** by chiral chromatography separation. (3*S*,5*R*)-**12**[19] was found to be a highly potent inhibitor of rh-renin (IC_{50} = 0.003 μM), while the distomer (3*R*,5*S*)-**12** was ~200-fold less active in vitro (Table 1). The crystal structure of (3*S*,5*R*)-**12** bound to rh-renin (Figure 4c) revealed a perfect overlay with enzyme–bound **9** and moreover confirmed the flexible methoxybutyl side chain to penetrate deeply into the S_3^{sp} cavity in an extended conformation. The terminal methoxy group was positioned at the bottom of the channel, closely overlaying with the side chain methoxy of **1** and forming a H-bond to the Tyr_{14} backbone nitrogen. Limited SAR investigation by modifying P_3^{sp} showed its length and shape to be critical for binding affinity, with the methoxybutyl residue leading to maximal potency (data not shown).

Finally, (*rac*)**-15** lacking the C5 prime site extension was synthesized (Scheme 4) and tested in the FRET biochemical assay (IC_{50} of 4.0 μM, Table 1) in order to estimate the relative contributions of the tolylsulfonamide moiety vs the P_3^{sp} side chain for inhibitory binding affinity in comparison to the most potent compound (3*S*,5*R*)**-12** of this novel class of renin inhibitors. The impact of adding the P_3^{sp} methoxybutyl side appeared to be very significant as suggested by the more than 100-fold difference in the IC_{50} for (*rac*)**-15** compared to the complete lack of renin inhibition at 100 μM in the biochemical assay for (*rac*)**-6** (Table 1) but is less pronounced for tolylsulfonamide analogues (*rac*)**-9** vs (*rac*)**-12** (23-fold difference in IC_{50}s). Most notably, (*rac*)**-15** was found to be 1000-fold less potent than (3*S*,5*R*)**-12**, the latter bearing the C5 sulfonamide portion. This result corroborates previous findings[10b] indicating the importance of efficient ligand–protein interactions at the extended prime site for strong inhibitory activity for different classes of S_3–S_1 topological peptidomimetic renin inhibitors.

Table 1. *In vitro* inhibition of rh-renin.[a]

	(*rac*)**-5**	(*rac*)**-6**	(*rac*)**-9**	(*rac*)**-12**	(3*S*,5*R*)**-12**	(3*R*,5*S*)**-12**	(*rac*)**-15**
IC_{50} (μM)[a]	1.2	>100[b]	0.09	0.004	0.003	0.5	4.0
StdDev	±0.5		±0.05	±0.002	±0.002	±0.2	±2.5

[a]Half–maximal inhibition of rh-renin in a fluorescence–polarization enzymatic assay using (RE(EDANS)IHPFHLVIHTK(Dabcyl)R as the substrate in 50 mM Tris-HCl buffer pH 7.4.[16] Data represent mean values from ≥4 independent experiments. [b]0% inhibition at the maximal 100 μM ligand concentration tested.

We explored in more detail the preclinical profile of (3*S*,5*R*)-**12** in order to assess its lead potential for further optimization. Potency toward renin was reduced only ~10-fold when measured in the presence of human plasma (plasma renin IC_{50} = 0.025 μM).[8,10a] Also, (3*S*,5*R*)-**12** was highly selective against a panel of recombinant human aspartic proteases comprising pepsins A and C, cathepsins D and E, as well as BACE 1 and BACE 2 (all IC_{50}s >30 μM). The lead compound (3*S*,5*R*)-**12** did show time dependent inhibition of CYP3A4 (k_{obs} 0.073 min^{-1}). In fed Sprague–Dawley rats, oral bioavailability was moderate (18%) with plasma levels exceeding the in vitro IC_{50} for >6 hours (doses: 2 mg/kg i.v. and 6 mg/kg p.o.; estimated $t_{1/2}$ = 2.3 hours; Cl_P = 2.6 L/h/kg; Vd_{ss} = 5.3 L/kg; oral C_{max} = 222 nM, oral $AUC_{(0\text{-}24\ h)}$ = 750 nM·h). A single oral dose (6 mg/kg and 30 mg/kg) given to telemetered hypertensive double-transgenic rats (dTGRs)[24] resulted in a maximal dose-dependent reduction of mean arterial blood pressure of -28 and -58 mmHg, respectively, and a 50% recovery time to pre-treatment baseline levels of 3.1 and 7.8 h, respectively.

In summary, we have successfully applied an integrated hit finding approach based on multiple screening efforts by in silico computational, biophysical and biochemical methods to identify a novel class of topological peptidomimetic renin inhibitors bearing a center 3,5-disubstituted piperidine and a tricyclic P_3–P_1 unit. Merging the information gained from crystal structures for two rh-renin bound low-affinity fragments identified by NMR from a target-biased library, as well as for a biochemical assay HTS hit enabled the rapid design of the in vitro highly potent, selective (3*S*,5*R*)-**12** as the preclinical lead. The novel TS surrogate inhibitor displayed an unprecedented binding mode to a non-substrate topography of the prime site of rh-renin in a closed flap conformation. This series warrants further exploration due to the attractive oral blood pressure lowering efficacy for (3*S*,5*R*)-**12** in the dTGR model.

EXPERIMENTAL SECTION

Chemistry General Procedures. Unless otherwise specified, all solvents and reagents were obtained from commercial suppliers and used without further drying or purification. All reactions were performed under nitrogen atmosphere, unless otherwise noted. Normal-phase flash chromatography was performed using Merck silica gel 60 (230-400 mesh). Purity was determined by analytical HPLC from the integration of the area under the UV absorption curve at λ =254 nm or 214 nm signals. ^{1}H NMR spectra were recorded on 400 MHz or 300 MHz spectrometers; chemical shift (δ) values were referenced to tetramethylsilane as internal standard and were reported as follows: (δ) shift (multiplicity, coupling constants, proton count). Mass spectral analyses were accomplished using electrospray (ESI) ionization techniques. High-resolution mass spectrum analyses (HR–MS) were performed on an APEX-III 9.4T FT–MS.

Abbreviations. U9-BBN: 9-borabicyclo[3.3.1]nonane; Boc: tert-butoxycarbonyl; $(Boc)_2O$: di-tert-butyl dicarbonate; DMAP: 4-(dimethylamino)pyridine; DIPEA: ethyldiisopropylamine; DMF,: dimethyl formamide; DMA: dimethyl acetamide; DMAP: 4-dimethylamino pyridine; EEDQ: 2-ethoxy-1-ethoxycarbonyl-1,2-dihydroquinoline; Et_3N: triethylamine; EtOAc: ethyl acetate; EtOH: ethyl alcohol; Fmoc: fluorenylmethoxycarbonyl; HATU: O-(7-azabenzotriazol-1-yl)-N,N,N´N´-tetramethyluronium hexafluorophosphate; HCTU: O-(6-chlorobenzotriazol-1-yl)-N,N,N´N´-tetramethyluronium hexafluorophosphate; HMPA: hexamethylphosporamide; HOBt: 1-hydroxybenzotriazole; LDA: lithium diisopropylamide; PyBOP: (benzotriazol-1-yloxy)tripyrrolidinophosphonium hexafluorophosphate; Nishimura catalyst: mixed Rh/Pt-oxide

(Umicore AG, Degussa GmbH); RT: room temperature; Suc: succinimide; TBME: tert-butylmethyl ether; TFA: trifluoroacetic acid; TMS: trimethylsilyl.

Preparation of *(rac)*-6 (Scheme 1)

9H-Xanthene-9-carboxylic acid benzylamide. To a solution of 9H-xanthene-9-carboxylic acid (10 g, 44.2 mmol) in CH_2Cl_2 (100 mL) were added EEDQ (16.4 g, 66 mmol) and, after 30 min, benzylamine (19.3 mL, 177 mmol). The mixture was stirred at RT overnight. The mixture was washed with aq. 1 N HCl, saturated aq. $NaHCO_3$ and brine. The organic layer was dried over Na_2SO_4, filtered and concentrated under reduced pressure to give a solid. Ethyl acetate was added and the suspension was stirred for 30 min and filtered. The precipitate was washed with ethyl acetate and dried under vacuum overnight to give the title compound as a white solid (5.6 g, 40%). 1H-NMR (400 MHz, DMSO-d_6): δ 4.25 (d, *J*= 8.4 Hz, 2 H), 5.01 (s, 1H), 7.10-7.38 (m, 13H), 8.95 (t, *J*= 8.4 Hz, 1 H) ppm. MS (ESI) m/z 316 $[M+H]^+$.

Benzyl-(9H-xanthen-9-ylmethyl)-amine. Aluminium trichloride (7.1 g, 53 mmol) was added in small portions to a suspension of $LiAlH_4$ (6.7 g, 178 mmol) in THF (30 mL) at 0 °C. The mixture was stirred for 10 min at 0 °C, before a solution of 9H-xanthene-9-carboxylic acid benzylamide (5.6 g, 17.8 mmol) in THF (26 mL) was added dropwise at 0 °C. The mixture was heated to 50 °C for 5 h before it was cooled to RT and treated with aq. NaOH (15%) and filtered. The filter cake was washed with ethyl acetate, and the solution was washed with saturated $NaHCO_3$. The aq. phase was extracted three times with ethyl acetate and the combined organic phases were dried over Na_2SO_4, filtered and evaporated. The resulting residue was purified by flash chromatography on silica gel (eluent: CH_2Cl_2 to CH_2Cl_2/MeOH 98:2) to give the title

compound as a yellow oil (3.8 g, 72%). 1H-NMR (400 MHz, DMSO- d_6): δ 2.65 (d, *J*= 9.5 Hz, 2 H), 3.62 (s, 2 H), 4.16 (t, *J*= 8.4 Hz, 1 H), 7.1-7.19 (m, 13 H) ppm. MS (ESI) m/z 302 $[M+H]^+$.

C-(9H-Xanthen-9-yl)-methylamine (8). A mixture of benzyl-(9H-xanthen-9-ylmethyl)-amine (3.8 g, 12.6 mmol), palladium on charcoal (1g, 10%) and ethanol (40 mL) was stirred at atmospheric pressure under hydrogen overnight. The mixture was filtered and the solvent evaporated to yield the title compound **8** as a yellow oil (2.6 g, 99%). 1H-NMR (400 MHz, DMSO-d_6): δ 2.74 (d, *J*= 8.9 Hz, 2 H), 3.33 (overlap with HDO signal, 2 H), 3.62 (s, 2 H), 3.92 (t, *J*= 8.4 Hz, 1 H), 7.14 (t, *J*= 7.9 Hz, 4 H), 7.28 (t, *J*= 7.9 Hz, 2 H), 7.39 (d, *J*= 6.2 Hz, 2 H) ppm. MS (ESI) m/z 212 $[M+H]^+$.

(*rac*)-3-{[9H-xanthen-9-ylmethyl]-carbamoyl}-piperidine-1-carboxylic acid tert-butyl ester. To C-[9H-xanthen-9-yl]-methylamine (**8**) (175 mg, 0.8 mmol) in CH_3CN (1.5 mL) was added PyBOP (517 mg, 0.96 mmol) and after 30 min racemic piperidine-1,3-dicarboxylic acid 1-tert-butyl ester (276 mg, 1.2 mmol) and triethylamine (1.1 mL) in CH_3CN (1.5 mL). The reaction mixture was stirred at RT overnight, before sat. $NaHCO_3$ was added. The aq. layer was extracted with dichloromethane. The organic layer was dried over Na_2SO_4, filtered and concentrated under reduced pressure to give a residue, which was purifed by flash chromatography on silica gel (eluent: hexane/ethyl acetate 9:1 to 1:1) to give the title compound as a colorless solid (276 mg, 79%). 1H-NMR (400 MHz, DMSO-d_6): δ 1.22-1.36 (m, 1 H), 1.42 (s, 9 H), 1.62 (bd, *J*= 11.6 Hz, 1 H), 1.78 (bd, *J*= 12.6 Hz, 1 H), 2.21 (bt, *J*= 11.8 Hz, 1 H), 2.58-2.74 (m, 1 H), 3.2 (bs, 2 H), 3.83-3.98 (m, 2 H), 4.13 (t, *J*= 6.3 Hz, 1 H), 7.11-7.18 (m, 4 H), 7.24-7.33 (m, 4 H), 8.07 (bt, *J*= 6.2 Hz, 1 H) ppm. MS (ESI) m/z 423 $[M+H]^+$.

((*rac*)-Piperidine-3-carboxylic acid [9H-xanthen-9-ylmethyl]-amide (6). To a mixture of racemic 3-{[9H-xanthen-9-ylmethyl]-carbamoyl}-piperidine-1-carboxylic acid tert-butyl ester

(100 mg, 0.3 mmol) in dioxane (2 mL) was added HCl (4M in dioxane, 1 mL) and the reaction mixture was stirred for 3 h at RT before it was treated with sat. $NaHCO_3$ and extracted with dichloromethane. The organic layer was dried over Na_2SO_4, filtered and concentrated under reduced pressure to give *(rac)*-**6** as a colorless solid (54 mg, 56%). 1H-NMR (400 MHz, DMSO-d_6): δ 1.11-1.55 (m, 3 H), 1.62-1.78 (m, 1 H), 2.06-2.19 (m, 1 H), 2.32-2.44 (m, 2 H), 2.79 (t, *J*= 15 Hz, 2 H), 3.16 (t, *J*= 6.3 Hz, 2 H), 3.32 (bs, 1 H), 4.1 (t, *J*= 6.7 Hz, 1 H), 7.04-7.17 (m, 4 H), 7.21-7.29 (m, 4 H), 7.98 (bt, *J*= 7.1 Hz, 1 H) ppm. MS (ESI) m/z 409 $[M+H]^+$. t_R (HPLC, Nucleosil C18; 10-90% CH_3CN+0.1%TFA/H_2O+0.1%TFA for 11 min, flow 1.5 mL/min): 4.1 min. HRMS calcd. for $C_{20}H_{22}N_2O_2$ $(M+H)^+$ 323.1754 and observed 323.1754.

Preparation of *(rac)*-15 (Scheme 4)

9H-Xanthene-9-carboxylic acid methyl ester. To a suspension of 9H-xanthene-9-carboxylic acid (20 g, 88.4 mmol) and Cs_2CO_3 (34.5 g, 106 mmol) in dimethyl formamide (300 mL), methyl iodide (8.3 mL, 133 mmol) was added dropwise at RT. The reaction was stirred for 1h before it was quenched with water and extracted with diethyl ether. The organic phase was washed twice with water and brine, dried over Na_2SO_4, filtered and evaporated to yield the title compound as a yellow solid (20.6 g, 97%). 1H-NMR (400 MHz, DMSO-d_6): δ 3.59 (s, 3 H), 5.13 (s, 1 H), 7.13-7.21 (m, 4 H), 7.32-7.4 (m, 4 H) ppm.

9-But-3-enyl-9H-xanthene-9-carboxylic acid methyl ester. 9H-Xanthene-9-carboxylic acid methyl ester (10 g, 41.7 mmol) was added dropwise at -78 °C to a freshly prepared solution of lithium diisopropyl amine (43.7 mmol) in THF (200 mL) and the mixture was stirred at -78 °C for 30 min. HMPA (14.5 mL) was added and stirring was continued at -78 °C before 4-bromo-1-butene (8.45 mL, 83 mmol) was added. After further stirring at -78 °C for 1 h the reaction was

warmed to 0 °C and, after 3 hours, quenched through the addition of sat. aq. NH_4Cl and extracted with diethyl ether. The organic phase was washed with water and brine, dried over Na_2SO_4, filtered and evaporated to give a residue, which was purifed by flash chromatography on silica gel (eluent: hexane/ethyl acetate 98:2 to 9:1) to give the title compound as a light yellow solid (9.96 g, 81%). 1H-NMR (400 MHz, DMSO-d_6): δ 1.42-1.53 (m, 2 H), 2.36-2.39 (m, 2 H), 3.59 (s, 3 H), 4.8 (d, *J*= 8.9 Hz, 1 H), 4.83 (s, 1 H), 5.56-5.7 (m, 1 H), 7.15 (t, *J*= 7.4 Hz, 4 H), 7.24 (d, *J*= 9.5 Hz, 2 H), 7.38 (t, *J*= 7.9 Hz, 2 H) ppm.

9-(4-Hydroxy-butyl)-9H-xanthene-9-carboxylic acid methyl ester. A solution of 9-but-3-enyl-9H-xanthene-9-carboxylic acid methyl ester (9.96 g, 33.8 mmol) in THF (85 mL) was added to 9-borabicyclo[3.3.1]nonane (8.3 g, 67.7 mmol) under argon and stirred at 40 °C for 5 min until a clear solution was obtained. The mixture was stirred at RT for 1 h before it was cooled to 0 °C and water (5 mL) was added dropwise. The reaction was kept at 0 °C while aq. H_2O_2 (30%, 21.6 mL, 210 mmol) and subsequently aq. NaOH (2 M, 68 mL) were added dropwise. The resulting mixture was stirred at RT for 30 min, before it was diluted with ethyl acetate and washed with aq. $NaHSO_4$, $NaHSO_3$, $NaHCO_3$ and NaCl. The organic phase was dried over Na_2SO_4, filtered and evaporated. The resulting solid was purified by flash chromatography on silica gel (eluent: hexane/ethyl acetate 4:1 to hexane/ ethyl acetate 1:1) to give the title compound as a white solid (6.6 g, 63%). 1H-NMR (400 MHz, DMSO-d_6): δ 0.66-0.8 (m, 2 H), 1.25 (t, *J*= 5.8 Hz, 2 H), 2.22-2.29 (m, 2 H), 3.12-3.19 (m, 2H) 3.57 (s, 3 H), 4.12 (t, *J*= 5.3 Hz, 1 H), 7.12-7.18 (m, 4 H), 7.24 (d, *J*= 9.5 Hz, 2 H), 7.36 (t, *J*= 7.9 Hz, 2 H) ppm. MS (ESI) m/z 313 $[M+H]^+$.

9-(4-Methoxy-butyl)-9H-xanthene-9-carboxylic acid methyl ester, 14. NaH (55%, 1.13 g, 25.9 mmol) was added to a solution of 9-(4-hydroxy-butyl)-9H-xanthene-9-carboxylic acid methyl ester (5.4 g, 17.3 mmol) and methyl iodide (3.3 mL, 52 mmol) in DMF (50 mL) at 0 °C.

The mixture was stirred at RT overnight before it was quenched with water and extracted with ethyl acetate. The organic phase was dried over Na_2SO_4, filtered and evaporated to give **14** as an oil containing ~15% DMF (5.8 g, 15% DMF, 90%). 1H-NMR (400 MHz, DMSO-d_6): δ 0.64-0.79 (m, 2 H), 1.26-1.38 m, 2 H), 2.23-2.29 (m, 2 H), 3.06 (s, 3 H), 3.07-3.13 (m, 2H) 3.58 (s, 3 H), 7.13-7.18 (m, 4 H), 7.22 (d, *J*= 9.5 Hz, 2 H), 7.35 (t, *J*= 7.9 Hz, 2 H) ppm. MS (ESI) m/z 327 $[M+H]^+$.

9-(4-Methoxy-butyl)-9H-xanthene-9-carboxylic acid. To a solution of 9-(4-methoxy-butyl)-9H-xanthene-9-carboxylic acid methyl ester (5.87 g, 15.2 mmol) in dioxane (15 mL) 2 M NaOH (15 mL) was added and the mixture was stirred at 60 °C before the solvents were evaporated. The residue was dissolved in dichloromethane and washed with 1 N HCl, water and brine. The organic phase was dried over Na_2SO_4, filtered and evaporated to give the title compound as an oil (5.7 g), which was directly used in the next step.

9-(4-Methoxy-butyl)-9H-xanthene-9-carboxylic acid benzylamide. Benzylamine (3.35 mL, 30.7 mmol) and TEA (21.3 mL) in DMF (20 mL) were added at 0 °C to PyBOP (9.6 g, 18.4 mmol) and 9-(4-methoxy-butyl)-9H-xanthene-9-carboxylic acid (5.7 g, 18.2 mmol) in DMF (40 mL). The mixture was stirred at RT overnight before it was treated with aq. sat. $NaHCO_3$ and extracted with dichloromethane. The organic phase was dried over Na_2SO_4, filtered and evaporated. The resulting solid was purified by flash chromatography on silica gel (eluent: hexane/ethyl acetate 2:1 to hexane/ ethyl acetate 1:1) to give the title compound as a white solid (5.1 g, 83% over two steps). 1H-NMR (300 MHz, DMSO-d_6): δ 0.6-0.77 (m, 2 H), 1.21-1.32 m, 2 H), 2.08-2.17 (m, 2 H), 3.02 (s, 3 H), 3.02-3.09 (m, 2H) 4.18 (d, *J*= 6.3 Hz, 2 H), 6.96-7.32 (m, 13 H), 7.8 (t, *J*= 6.3 Hz, 2 H) ppm. MS (ESI) m/z 402 $[M+H]^+$.

Benzyl-[9-(4-methoxy-butyl)-9H-xanthen-9-ylmethyl]-amine. A solution of 9-(4-methoxy-butyl)-9H-xanthene-9-carboxylic acid benzylamide (5 g, 12.5 mmol) and $BH_3 \cdot (CH_3)_2S$ (2 M, 15.6 mL) in THF (13 mL) was heated in the microwave for 15 min at 150 °C. The reaction mixture was carefully quenched with water, before 1 N HCl was added. The mixture was neutralized with aq. sat. $NaHCO_3$ after stirring at RT overnight and extracted with ethyl acetate. The organic phase was dried over $MgSO_4$, filtered and evaporated. The resulting solid was purified by flash chromatography on silica gel (eluent: dichloromethane to dichloromethane/ MeOH 95:5) to give the title compound as an oil (4.1 g, 86%). 1H-NMR (300 MHz, DMSO-d_6): δ 0.7-0.83 (m, 2 H), 1.21-1.36 m, 2 H), 1.88-1.99 (m, 2 H), 2.85-2.91 (m, 2 H), 3.02 (s, 3 H), 3.02-3.09 (m, 2H), 3.4-3.42 (m, 2H), 6.92-7.39 (m, 13 H) ppm. MS (ESI) m/z 388 $[M+H]^+$.

C-[9-(4-Methoxy-butyl)-9H-xanthen-9-yl]-methylamine (13). A mixture of benzyl-[9-(4-methoxy-butyl)-9H-xanthen-9-ylmethyl]-amine (4 g, 10.3 mmol), palladium on charcoal (0.4 g, 10%) and ethanol (40mL) was stirred at atmospheric pressure under hydrogen overnight. The mixture was filtered and the solvent evaporated to yield **13** as a yellow oil (2.4 g, 78%). 1H-NMR (400 MHz, DMSO-d_6): δ 0.74-0.87 (m, 2 H), 1.32-1.39 m, 2 H), 1.91-1.99 (m, 2 H), 2.98 (s, 2 H), 3.08 (s, 3 H), 3.09-3.14 (m, 2H), 7.05 (d, *J*= 9.4 Hz, 2 H), 7.15 (t, *J*= 7.9 Hz, 2 H), 7.22 (t, *J*= 7.4 Hz, 2 H), 7.44 (d, *J*= 9.4 Hz, 2 H) ppm. MS (ESI) m/z 298 $[M+H]^+$. HRMS calcd. for $C_{19}H_{23}NO_2$ $(M+H)^+$ 298.1802 and observed 298.1802.

(*rac*)-3-{[9-(4-Methoxy-butyl)-9H-xanthen-9-ylmethyl]-carbamoyl}-piperidine-1-carboxylic acid tert-butyl ester. To a stirred, ice-cooled mixture of racemic piperidine-1,3-dicarboxylic acid 1-tert-butyl ester (231 mg, 1 mmol) in CH_2Cl_2 (1.5 mL) was added HCTU (342 mg, 0.8 mmol) and after 5 min C-[9-(4-methoxy-butyl)-9H-xanthen-9-yl]-methylamine (**13**) (200 mg, 0.67 mmol) and triethylamine (0.9 mL) in CH_3CN (1.5 mL). The reaction mixture was stirred at

RT overnight, before sat. $NaHCO_3$ was added. The aq. layer was extracted with dichloromethane. The organic layer was dried over Na_2SO_4, filtered and concentrated under reduced pressure to give a residue, which was purified by flash chromatography on silica gel (eluent: hexane/ethyl acetate 1:1 to 0:1) to give the title compound as a colorless solid (298 mg, 87%). 1H-NMR (400 MHz, DMSO-d_6): δ 0.78-0.86 (m, 2 H), 1.06-1.19 (m, 2 H), 1.31-1.49 (m, 4 H), 1.39 (s, 9 H), 1.98-2.05 (m, 2 H), 2.06-2.18 (m, 1 H), 2.38-2.6 (overlap with DMSO signal, m, 4H), 3.06 (s, 3 H), 3.14 (t, *J*= 5.8 Hz, 2 H), 3.31 (bs, 2 H), 3.78-3.86 (m, 1 H), 7.02-7.06 (m, 2 H), 7.07-7.14 (m, 2 H), 7.24 (t, *J*= 9.5 Hz, 2 H), 7.42 (t, *J*= 8.4 Hz, 2 H), 7.53 (bs, 1 H) ppm. MS (ESI) m/z 453 $[M+H-{}^tBu]^+$.

(*rac*)-Piperidine-3-carboxylic acid [9-(4-methoxy-butyl)-9H-xanthen-9-ylmethyl]-amide (15). To a mixture of racemic 3-{[9-(4-methoxy-butyl)-9H-xanthen-9-ylmethyl]-carbamoyl}-piperidine-1-carboxylic acid tert-butyl ester (260 mg, 0.5 mmol) in dioxane (3 mL) was added HCl (4M in dioxane, 1 mL) and the reaction mixture was stirred for 3 h at RT before it was treated with sat. $NaHCO_3$ and extracted with dichloromethane. The organic layer was dried over Na_2SO_4, filtered and concentrated under reduced pressure to give *(rac)*-**15** as a yellow solid (175 mg, 84%). 1H-NMR (400 MHz, DMSO-d_6): δ 0.71-0.85 (m, 2 H), 1.04-1.22 (m, 6 H), 1.96-2.08 (m, 4 H), 2.25-2.38 (m, 2 H), 2.55-2.64 (m, 1 H), 3.07 (s, 3 H), 3.12 (t, *J*= 5.3 Hz, 2 H), 3.51-3.69 (m, 2 H), 7.02 (d, *J*= 8.4 Hz, 2 H), 7.06-7.14 (m, 2 H), 7.22-7.28 (m, 2 H), 7.42-7.48 (m, 2 H), 7.65 (bs, 1 H) ppm. MS (ESI) m/z 409 $[M+H]^+$; t_R (HPLC, Nucleosil C18; 10-100% CH_3CN+0.1%TFA/H_2O+0.1%TFA for 8 min, flow 1.5mL/min): 4.4 min. HRMS calcd. for $C_{25}H_{32}N_2O_3$ $(M+H)^+$ 409.2486 and observed 409.2486.

Preparation of *(rac)*-11 (Scheme 2 and Scheme S1)

(*rac,cis*)-5-tert-Butoxycarbonylamino-1-piperidine-3-carboxylic acid. A mixture of 5-tert-butoxycarbonylamino-nicotinic acid **10** (380 g, 1.59 mol), Nishimura's catalyst [mixed Rh/Pt oxide] (38 g) in distilled H_2O (7.0 L) and 25% aqueous NH_4OH solution (1.7 L) was shaken at RT under hydrogen atmosphere for 24 h. After addition of a second portion of the Nishimura catalyst (38 g) the reaction was continued for 21 h. After addition of a third portion of catalyst (38 g) shaking was continued for 24 h. The reaction mixture was filtered through a pressure filter and the filter cake was washed three times with 0.5 L of water. The volume of the filtrate was reduced *in vacuo* to 2 L and the remaining suspension was cooled to 0 °C and filtered to yield the pure (*rac,cis*)-5-tert-butoxycarbonylamino-1-piperidine-3-carboxylic acid as a white powder (155 g, 40%). 1H-NMR (400 MHz, D_2O): δ 1.39 (s, 9 H), 1.48 (m, 1 H), 2.25 (m, 1 H), 2.57-2.69 (m, 2 H), 2.82 (m, 1 H), 3.38-3.50 (m, 2 H), 3.74 (m, 1H) ppm. MS (ESI) m/z 245.1 [M+H]+. Elemental analysis: calc. for $C_{11}H_{20}N_2O_4$: C 54.08, H 8.25, N 11.47 found: C 54.13, H 8.03, N 11.34. Evaporation and recrystallization of the mother liquor gave 50 g of a mixture of (*rac,trans*)- and (*rac,cis*)-5-tert-butoxycarbonylamino-1-piperidine-3-carboxylic acid in a *trans-cis* ratio of 78:22.

(*rac,cis*)-5-tert-Butoxycarbonylamino-piperidine-1,3-dicarboxylic acid 1-(9H-fluoren-9-ylmethyl) ester (11). To a stirred mixture of racemic cis-5-tert-butoxycarbonylamino-1-piperidine-3-carboxylic acid (120 g, 0.46 mol), $NaHCO_3$ (38.6 g, 0.46 mol), distilled H_2O (1.2 L) and THF (1.2 L), N-(9-fluorenylmethoxycarbonyloxy)-succinimide (186 g, 0.55 mol) was added in several portions. The reaction mixture was stirred for 22 h at RT. After addition of 45 g of $NaHCO_3$ (to adjust the pH of the acqueous to 7.5) and N-(9-fluorenylmethoxycarbonyloxy)-succinimide (30 g, 0.089 mol) stirring was continued for 4 h. The volatiles were evaporated and the residue was extracted with TBME (3x 1L). The pH value of the aq. phase was then adjusted

to 6.4 by the addition of 1M aq. HCl. The resulting suspension was filtered, washed with three portions of water (1 L) and dried at 50 °C *in vacuo* to obtain (*rac,cis*)-**11** as a white powder (187 g, 88%). 1H-NMR (400 MHz, DMSO-d_6, broadened signals due to rotamers): δ 1.41 (s, 9 H), 2.04 (bs, 1 H), 2.22-2.42 (m, 1 H), 2.64 (bs, 1 H), 3.2-3.43 (m, 3 H), 3.98-4.22 (m, 2 H), 4.3 (bs, 2 H), 4.4 (bs, 1 H), 6.99 (bs, 1 H), 7.36-7.39 (m, 2 H), 7.4-7.43 (m, 2 H), 7.65 (bs, 2 H), 7.92 (d, *J*= 9.4 Hz, 2 H) ppm. t_R (HPLC, Nucleosil C18, 5-100% CH_3CN+0.1%TFA / H_2O+0.1%TFA for 8 min, 100% CH_3CN+0.1%TFA for 2 min, flow 1.5mL/min): 6.64 min. MS (ESI) m/z 467 [M+H]+. HRMS calcd. for $C_{26}H_{30}N_2O_6$ $(M+H)^+$: 467.2177; found 467.2176. Elemental analysis: calc. for $C_{26}H_{30}N_2O_6$: C 66.94, H 6.48, N 6.00 found: C 66.74, H 6.47, N 5.88.

Preparation of (3S,5R)-11 and (3R,5S)-11

(*rac,cis*)-5-tert-Butoxycarbonylamino-piperidine-1,3-dicarboxylic acid 1-(9H-fluoren-9-ylmethyl) ester, *(rac)*-**11** (9.81 g) was separated into its enantiomers using preparative chiral chromatography (chiral HPLC, Chiralcel OJ, 50x10cm, 20 μm, 60% hexane +0.1% TFA / 40% ethanol +0.1% TFA, flow 100 mL/min; detection: UV at 210 nm.

(3S,5R)-5-tert-Butoxycarbonylamino-piperidine-1,3-dicarboxylic acid 1-(9H-fluoren-9-ylmethyl) ester, (3S,5R)-**11** was isolated in 105% yield (5.18 g, containing TFA-salts as minor contamination) as peak 1; the enatiomeric purity was determined to be ee >99%. 1H-NMR (400 MHz, DMSO-d_6): δ 1.40 (s, 9 H), 2.06 (bs, 1 H), 2.18-2.52 (m, 2 H), 2.62 (m, 1 H), 3.14-3.42 (m, 2 H), 3.92-4.45 (m, 5 H), 6.93 (bs, 1 H), 7.30 (m, 2 H), 7.38 (m, 2 H), 7.62 (bs, 2 H), 7.83 (d, 2 H), 12.48 (bs, 1H) ppm; t_R (chiral HPLC, Chiralcel OJ 250x4.6 mm, 10 μm; 80% n-hexane +0.1%TFA / 20% ethanol +0.1%TFA, flow 1mL/min): 8.9 min; MS (ESI) m/z 465.3 $[M-H]^-$;

$[\alpha]^{25}_{D}$ -8.2 (c 1.0, MeOH); Elemental analysis: calc. for $C_{26}H_{30}N_2O_6$: C 66.94, H 6.48, N 6.00 found: C 66.61, H 6.40, N 5.79.

(3*S*,4*R*)-**11** was used as the starting material for the preparation of (3*S*,4*R*)-**5** as described below. The absolute configuration of crystalline (3*S*,4*R*)-**5** was determined by small molecule X-ray diffraction (vide infra).

(3R,5S)-5-tert-Butoxycarbonylamino-piperidine-1,3-dicarboxylic acid 1-(9H-fluoren-9-ylmethyl) ester, (3R,5S)-**11** was isolated in 83% yield (4.06 g) as peak 2; the enantiomeric purity was determined to be ee >99%. 1H-NMR (400 MHz, $DMSOd_6$): δ 1.40 (s, 9 H), 2.04 (bs, 1 H), 2.17-2.52 (m, 2 H), 2.62 (m, 1 H), 3.14-3.41 (m, 2 H), 3.92-4.46 (m, 5 H), 6.92 (bs, 1 H), 7.31 (m, 2 H), 7.38 (m, 2 H), 7.61 (m, 2 H), 7.82 (d, 2 H), 12.42 (bs, 1H) ppm; t_R (chiral HPLC, Chiralcel OJ 250x4.6 mm, 10 μm; 80% n-hexane +0.1%TFA / 20% ethanol +0.1%TFA, flow 1mL/min): 19.3 min; MS (ESI) m/z 465.3 $[M-H]^-$; $[\alpha]^{25}_{D}$ +7.4 (c 1.0, MeOH); Elemental analysis: calc. for $C_{26}H_{30}N_2O_6$: C 66.94, H 6.48, N 6.00 found: C 66.74, H 6.47, N 5.88.

Preparation of *(rac)*-9 (Scheme 2 and Scheme S1)

(*rac,cis*)-5-Amino-piperidine-1,3-dicarboxylic acid 1-(9*H*-fluoren-9-ylmethyl) ester, hydrochloride salt. To a mixture of (*rac,cis*)-5-tert-butoxycarbonylamino-piperidine-1,3-dicarboxylic acid 1-(9H-fluoren-9-ylmethyl) ester, *(rac)*-**11**, (5.2 g, 11.1 mmol) in dioxane (28 mL), 4 M HCl in dioxane (28 mL, 111 mmol) was added and the reaction mixture was stirred for 16 h at RT. n-Hexane (50 mL) was added and the precipitate was filtered off, washed with n-hexane and dried *in vacuo* to afford the title compound as a white solid (4.3 g, 96%). 1H-NMR (400 MHz, DMSO-d_6, broadened signals due to rotamers): δ 2.05-2.45 (bm, 2 H), 2.6-2.78 (bm, 2 H), 3.02-3.2.9 (bm, 1 H), 4.08 (bs, 1 H), 4.2-4.5 (bm, 2 H), 4.32 (bs, 2 H), 4.4 (bs, 1 H), 7.32-

7.4 (m, 2 H), 7.43 (t, *J*= 7.9 Hz, 2 H), 7.65 (d, *J*= 9.2 Hz, 2 H), 7.92 (d, *J*= 8.4 Hz, 2 H), 8.28 (bs, 2 H) ppm. MS (ESI) m/z 367.4 $[M+H]^+$.

(*rac,cis*)-5-(Toluene-4-sulfonylamino)-piperidine-1,3-dicarboxylic acid 1-(9*H*-fluoren-9-ylmethyl) ester. To a stirred, ice-cooled mixture of (*rac,cis*)-5-amino-piperidine-1,3-dicarboxylic acid 1-(9*H*-fluoren-9-ylmethyl) ester, hydrochloride salt, (500 mg, 1.24 mmol), aq. 10% K_2CO_3 (5.2 mL) and dioxane (4 mL), 4-toluenesulfonyl chloride (284 mg, 1.5 mmol) was added in several portions at 0 °C and stirring was continued for 1h. The reaction mixture was diluted with ethyl acetate and then acidified with 2 M HCl. The aq. phase was extracted three times with ethyl acetate. After washing with brine, the combined organic extracts were dried (Na_2SO_4) and the solvent was evaporated *in vacuo* to afford the title compound as a white solid (347 mg, 54%). 1H-NMR (400 MHz, DMSO-d_6, broadened signals due to rotamers) δ 1.38 (bs, 1H), 1.89 (bs, 1 H), 2.09 (bs, 1 H), 2.22 (s, 1.5 H), 2.4 (s, 1.5 H), 2.64 (bs, 1 H), 2.85-3.16 (bm, 1 H), 3.29 (bs, 3 H), 3.92-4.1 (bm, 2 H), 4.12-4.32 (m, 3 H), 7.24-7.44 (m, 6 H), 7.54-7.64 (m, 2 H), 7.75 (bs, 2 H), 7.92 (bs, 2 H) ppm. MS (ESI) m/z 521.1 $[M-H]^-$.

(*rac,cis*)-3-(Toluene-4-sulfonylamino)-5-[(9*H*-xanthen-9-ylmethyl)-carbamoyl]-piperidine-1-carboxylic acid 9*H*-fluoren-9-ylmethyl ester. To a stirred, ice-cooled solution of (*rac-cis*)-5-(toluene-4-sulfonylamino)-piperidine-1,3-dicarboxylic acid 1-(9*H*-fluoren-9-ylmethyl) ester (739 mg, 1.42 mmol) in CH_2Cl_2 (6 mL), DIPEA (0.24 mL, 1.4 mmol) was added, followed by HCTU (656 mg, 1.55 mmol) in CH_3CN (6 mL). The mixture was stirred for 15 min at 0 °C. After the addition of C-(9*H*-xanthen-9-yl)-methylamine **8** (122 mg, 0.576 mmol), stirring was continued for 1 h at 0 °C and then for 14 h at RT. The suspension was filtered and the filtrate evaporated. The residue thus obtained was distributed between a saturated $NaHCO_3$ solution and ethyl acetate. The aq. layer was extracted with ethyl acetate. The combined organic layers were

washed with 2N HCl and brine, dried over Na_2SO_4, filtered and evaporated. Flash chromatography (CH_2Cl_2 to CH_2Cl_2/MeOH 9:1) afforded the title compound as a beige solid (708 mg) in 80% purity by HPLC. This material was directly used in the next step.

***(rac-cis)*-5-(Toluene-4-sulfonylamino)-piperidine-3-carboxylic acid (9*H*-xanthen-9-ylmethyl)-amide, *(rac)*-9**. A solution of *(rac-cis)*-3-(toluene-4-sulfonylamino)-5-[(9*H*-xanthen-9-ylmethyl)-carbamoyl]-piperidine-1-carboxylic acid 9*H*-fluoren-9-ylmethyl ester (708 mg) in CH_2Cl_2/piperidine (4:1, 14 mL) was stirred for 1 h at RT. After evaporation *in vacuo*, the residue was purified by flash chromatography (CH_2Cl_2/MeOH/NH_3 50:6:1) to afford ***(rac)*-9** as a white solid (21 mg, 5% over two steps). 1H-NMR (400 MHz, DMSO-d_6, broadened signals due to rotamers): δ 2.02-2.25 (m, 4 H), 2.4 (s, 3 H), 2.68-2.78 (m, 2 H), 2.82-2.92 (m, 1 H), 3.12-3.19 (m, 2 H), 3.26-3.78 (under HDO, m, 1 H), 4.07 (t, *J*= 5.8 Hz, 1 H), 7.03-7.18 (m, 3 H), 7.2-7.24 (m, 2 H), 7.25-7.32 (m, 2 H), 7.38-7.45 (m, 2 H), 7.61-7.75 (m, 3 H), 7.94 (t, *J*= 5.3 Hz, 1 H) ppm. MS (ESI) m/z 492 $[M+H]^+$. t_R (HPLC, Nucleosil C18; 10-100% CH_3CN+0.05%TFA/H_2O+0.05%TFA for 6 min, flow 1.5mL/min): 4.6 min.

Preparation of (*rac*)-12 (Scheme 3 and Scheme S1)

***(rac-cis)*-5-tert-Butoxycarbonylamino-3-{[9-(4-methoxy-butyl)-9*H*-xanthen-9-ylmethyl]-carbamoyl}-piperidine-1-carboxylic acid 9*H*-fluoren-9-ylmethyl ester.** A solution of HCTU (1.1 g, 2.7 mmol), DIEPA (0.37 mL, 2.1 mmol) and *(rac-cis)*-5-tert-butoxycarbonylamino-piperidine-1,3-dicarboxylic acid 1-(9*H*-fluoren-9-ylmethyl) ester, *(rac)*-**11**, (638 mg, 2.1 mmol) in dichloromethane / acetonitrile (5 mL / 5 mL) was stirred at RT for 30 min, at which time C-[9-(4-methoxy-butyl)-9H-xanthen-9-yl]-methylamine **13** (1 g, 2.1 mmol) was added. The mixture was stirred at RT overnight, before the resulting suspension was filtered and the filtrate

evaporated. The obtained residue was distributed between a saturated $NaHCO_3$ solution and ethyl acetate. The aq. layer was extracted with ethyl acetate. The combined organic layers were washed with 2N HCl and brine, dried over Na_2SO_4, filtered and evaporated. Flash chromatography (CH_2Cl_2 to CH_2Cl_2 / MeOH 95:5) afforded the title compound as a light yellow solid (669 mg, 42%). 1H-NMR (600 MHz, DMSO-d_6): δ 0.72-0.82 (m, 2 H), 0.95-1.04 (m, 1 H), 1.21-1.51 (m, 5 H), 1.95-2.07 (m, 3 H), 2.21-2.3 (m, 1 H), 2.32 (s, 3 H), 2.51-2.66 (m, 1 H), 2.75-2.89 (m, 1 H), 3.06 (s, 3 H), 3.09 (t, *J*= 5.2, 2 H), 3.45-3.62 (m, 2 H), 6.94-7.09 (m, 4 H), 7.14-7.24 (m, 2 H), 7.3-7.42 (m, 5 H), 7.56-7.69 (m, 3 H), ppm.

***(rac-cis)*-5-Amino-3-{[9-(4-methoxy-butyl)-9*H*-xanthen-9-ylmethyl]-carbamoyl}-piperidine-1-carboxylic acid 9*H*-fluoren-9-ylmethyl ester.** To a mixture of *(rac-cis)*-5-tert-butoxycarbonylamino-3-{[9-(4-methoxy-butyl)-9*H*-xanthen-9-ylmethyl]-carbamoyl}-piperidine-1-carboxylic acid 9*H*-fluoren-9-ylmethyl ester (600 mg, 0.8 mmol) in dioxane (6 mL), 4 M HCl in dioxane (0.6 mL) was added and the reaction mixture was stirred for 2 h at RT, when it was treated with sat. aq. $NaHCO_3$. The mixture was extracted with dichloromethane, washed with brine, dried over Na_2SO_4, filtered and evaporated. Flash chromatography (CH_2Cl_2 to CH_2Cl_2 / MeOH 95:5) affords the title compound as a beige solid (353 mg, 68%). 1H-NMR (400 MHz, DMSO-d_6, broadened signals due to rotamers) δ 0.74-0.83 (m, 2 H), 0.92-1.03 (m, 1 H), 1.14-1.21 (m, 2 H), 1.56-1.61 (m, 1 H), 1.99-2.1 (m, 2 H), 2.1-2.54 (bm, 4 H), 3.07 (s, 3 H), 3.15 (t, *J*= 5.4, 2 H), 3.29-3.38 (m, 3 H), 3.54-3.69 (m, 2 H), 3.61 (bs, 1 H), 3.73 (bs, 1 H), 4.22 (bs, 2 H), 6.9-7.16 (m, 4 H), 7.21-7.24 (m, 2 H), 7.31-7.39 (m, 2 H), 7.1-7.46 (m, 4 H), 7.54-7.62 (m, 3 H), 7.82-7.94 (m, 2 H) ppm. MS (ESI) m/z 646 $[M+H]^+$.

(rac-cis)-3-{[9-(4-Methoxy-butyl)-9H-xanthen-9-ylmethyl]-carbamoyl}-5-(toluene-4-sulfonylamino)-piperidine-1-carboxylic acid 9H-fluoren-9-ylmethyl ester. To a solution of

(rac-cis)-5-amino-3-{[9-(4-methoxy-butyl)-9*H*-xanthen-9-ylmethyl]-carbamoyl}-piperidine-1-carboxylic acid 9*H*-fluoren-9-ylmethyl ester (350 mg, 0.54 mmol) and 4-DMAP (13 mg, 0.11 mmol) in pyridine (5 mL) was added 4-toluenesulfonyl chloride (310 mg, 1.6 mmol) at 0 °C. The mixture was stirred at RT overnight, when water and 1 N HCl were added and extracted with dichloromethane. The organic phases were washed with brine, dried over Na_2SO_4, filtered and evaporated. The crude product (406 mg) was directly used in the next step.

(rac-cis)-5-(Toluene-4-sulfonylamino)-piperidine-3-carboxylic acid [9-(4-methoxy-butyl)-9H-xanthen-9-ylmethyl]-amide, (rac)-12. A solution of *(rac-cis)*-3-{[9-(4-methoxy-butyl)-9*H*-xanthen-9-ylmethyl]-carbamoyl}-5-(toluene-4-sulfonylamino)-piperidine-1-carboxylic acid 9*H*-fluoren-9-ylmethyl ester (400 mg) in CH_2Cl_2/piperidine (4:1, 4 mL) was stirred for 1 h at RT. After evaporation *in vacuo*, the residue was purified by flash chromatography (CH_2Cl_2/MeOH/NH_3 50:6:1) to afford the title compound, *(rac)*-**12**, as a light yellow solid (123 mg, 39% over two steps). For the NMR investigation, a small sample of the product was additionally purified by preparative HPLC (C18 column 250x40 mm, 20–100% CH_3CN + 0.1%TFA / H_2O + 0.1%TFA/ 30 min, flow 20 mL / min). The combined pure fractions were basified with solid K_2CO_3, CH_3CN was evaporated *in vacuo* and the residual aqueous layer was extracted twice with CH_2Cl_2. The combined organic extracts were dried over Na_2SO_4 and evaporated *in vacuo* to afford *(rac)*-**12** as a white solid. 1H-NMR (400 MHz, DMSO-d_6, broadened signals due to rotamers) δ 0.72-0.85 (m, 2 H), 1.07-1.17 (m, 1 H), 1.25-1.38 (m, 3 H), 1.82-2.03 (m, 5 H), 2.28-2.35 (m, 1 H), 2.36 (s, 3H), 2.58-2.66 (m, 1 H), 2.68-2.78 (m, 1H), 3.08 (s, 3 H), 3.10 (t, 2 H), 3.53-3.61 (m, 1 H), 6.93-7.09 (m, 4 H), 7.14-7.24 (m, 2 H), 7.28-7.40 (m, 5 H), 7.52 (d, 1 H), 7.62 (part of AB-system, 2H) ppm. t_R (HPLC, Nucleosil C18; 10-100%

CH_3CN+0.1%TFA/H_2O+0.1%TFA for 8 min, flow 1.5mL/min): 4.7 min. HRMS calcd. for $C_{32}H_{39}N_3O_5S$ $(M+H)^+$: 578.2683; found: 578.2683.

Preparation of (3S,5R)-12 and (3R,5S)-12 (Scheme 3 and Scheme S1)

(3S,5R)-5-(Toluene-4-sulfonylamino)-piperidine-3-carboxylic acid [9-(4-methoxy-butyl)-9*H*-xanthen-9-ylmethyl]-amide, (3S,5R)-12, was prepared from (3S,5R)-**11** as described for *(rac)*-12. 1H-NMR (400 MHz, DMSO-d_6) δ 0.72-0.82 (m, 2 H), 1.08-1.18 (m, 1 H), 1.28-1.4 (m, 3 H), 1.83-2.07 (m, 5 H), 2.29-2.36 (m, 1 H), 2.37 (s, 3H), 2.58-2.66 (m, 1 H), 2.69-2.79 (m, 1H), 3.08 (s, 3 H), 3.10 (t, 2 H), 3.38 (dd, 1 H), 3.58 (dd, 1 H), 6.95-7.1 (m, 4 H), 7.17-7.25 (m, 2 H), 7.31-7.42 (m, 5 H), 7.56 (d, 1 H), 7.64 (part of AB-system, 2H) ppm. t_R (HPLC, Nucleosil C18; 5-100% CH_3CN+0.1%TFA/H_2O+0.1%TFA for 8 min, flow 1.5mL/min): 5.4 min; MS (ESI) m/z 578.3 $[M+H]^+$; $[\alpha]^{25}_D$ -14.6 (c 1.0, MeOH); HRMS calcd. for $C_{32}H_{39}N_3O_5S$ $(M+H)^+$: 578.2683; found: 578.2683.

(3R,5S)-5-(Toluene-4-sulfonylamino)-piperidine-3-carboxylic acid [9-(4-methoxy-butyl)-9*H*-xanthen-9-ylmethyl]-amide, (3R,5S)-12, was prepared from (3R,5S)-**11** as described for *(rac)*-12. 1H-NMR (400 MHz, DMSO-d_6) δ 0.72-0.82 (m, 2 H), 1.08-1.19 (m, 1 H), 1.29-1.4 (m, 3 H), 1.83-2.06 (m, 5 H), 2.30-2.37 (m, 1 H), 2.38 (s, 3H), 2.60-2.67 (m, 1 H), 2.70-2.80 (m, 1H), 3.07 (s, 3 H), 3.10 (t, 2 H), 3.38 (dd, 1 H), 3.59 (dd, 1 H), 6.97-7.10 (m, 4 H), 7.18-7.26 (m, 2 H), 7.32-7.42 (m, 5 H), 7.57 (d, 1 H), 7.64 (part of AB-system, 2H) ppm; t_R (HPLC, Nucleosil C18; 5-100% CH_3CN+0.1%TFA/H_2O+0.1%TFA for 8 min, flow 1.5mL/min): 5.4 min; MS (ESI) m/z 578.4 $[M+H]^+$; $[\alpha]^{25}_D$ +13.7 (c 1.0, MeOH); HRMS calcd. for $C_{32}H_{39}N_3O_5S$ $(M+H)^+$: 578.2683; found: 578.2684.

Supporting Information. Description of experimental procedures for the solid phase synthesis of (*rac*-5) including synthesis schemes S1 and S2, determination of the absolute stereochemistry of (*3S,5R*)-**12**, experimental procedures for biological assays, protein–ligand NMR measurements, in vivo pharmacokinetics, in vivo pharmacology, X-ray crystallographic information for the rh-renin–inhibitor complexes. The crystal structures of rh-renin in complex with (rac)-3, (rac)-4, (3S,5R)-5, (rac)-6, (rac)-9 and (3S,5R)-12 have been deposited at the Protein Data Bank RSCB PDB with the PDB IDs 4GJ8, 4GJ9, 4GJA, 4GJB, 4GJC, and 4GJD, respectively. Crystallographic data (excluding structure factors) for (3*S*,5*R*)-**5** has been deposited with the Cambridge Crystallographic Data Centre as supplementary publication number CCDC 898747 (3*S*,5*R*)-**5**). Copies of the data can be obtained, free of charge, on application to CCDC, 12 Union Road, Cambridge CB2 1 EZ, UK [fax: +44-(0)1223-336033 or email: deposit@ccdc.cam.ac.uk]. This material is available free of charge via the internet at http://pubs.acs.org.

AUTHOR INFORMATION

Corresponding Author: *To whom correspondence should be addressed. Tel: +41 61 6961892. E-mail: daniel.baeschlin@novartis.com

Author Contributions

The manuscript was written through contributions of all authors. All authors have given approval to the final version of the manuscript.

Funding Sources

The authors declare no competing financial interest.

ACKNOWLEDGMENT

The authors thank Alexandra Löffler, Pierrick Richard, Hansjörg Haas, Marie-Hélène Bellance, Flavio Ossola, David Ruckstuhl, Paul Schultheiss, Florence Zink, Gabrielle Meder, Danielle Folio and Oliver Bruttger for their excellent technical assistance. Claude Hager is acknowledged for chiral separations, and Christian Guenat for HR–MS determination.

ABBREVIATIONS

RAAS, renin-angiotensin-aldosterone system; ACE, angiotensin converting enzyme; DRI, direct renin inhibitor; HTS, high-throughput screening; rh-renin, recombinant human renin; TS, transition state.

REFERENCES

(1) Kearney, P.M.; Whjelton, M.; Reynolds, K.; Muntner, P.; Whelton, P.K.; He, J. Global burden of hypertension: analysis of worldwide data. *Lancet* **2005**, 365, 217–223.

(2) Rosamond W.; Flegal K.; Friday G.; Furie K.; Go A.; Greenlund K.; Haase N.; Ho M.; Howard V.; Kissela B.; Kittner S.; Lloyd-Jones D.; McDermott M.; Meigs J.; Moy C.; Nichol G.; O'Donnell Ch. J.; Roger V.; Rumsfeld J.; Sorlie P.; Steinberger J.; Thom T.; Wasserthiel-Smoller S.; Hong Y. Heart disease and stroke statistics - 2007 update: a report from the American Heart Association Statistics Committee and Stroke Statistics Subcommittee. *Circulation* **2007**, *115*, e69–171.

(3) Scott, B. B.; McGeehan, G. M.; Harrison, R. R. Development of inhibitors of the aspartyl protease renin for the treatment of hypertension. *Curr. Prot. Pept. Sci.* **2006**, *7*, 241–254.

(4) Skeggs, L.T.; Kahn, J.R.; Lentz, K.; Shumway, N.P. The preparation, purification, and amino acid sequence of a polypeptide renin substrate. *J. Exp. Med*. **1957**, *106*, 439–453.

(5) (a) Ruddy M. C. Unmet Needs in Managing Hypertension: Potential Role of Direct Renin Inhibition. *Postgrad. Med.* **2010**, *122*, 203-212. (b) Volpe M, Pontremoli R, Borghi C. Direct renin inhibition: from pharmacological innovation to novel therapeutic. *High Blood Press Cardiovasc Prev.* **2011,** *18*, 93-105.

(6) Stanton, A.; Jensen, C.; Nussberger, J.; OBrien, E. Blood pressure lowering in essential hypertension with an oral renin inhibitor, aliskiren. *Hypertension* **2003**, 42, 1137–1143.

(7) Oh, B.-H.; Mitchell, J.; Herron, J. R.; Chung, J.; Khan, M.; Keefe, Deborah L. Aliskiren, an oral renin inhibitor, provides dose-dependent efficacy and sustained 24-hour blood pressure control in patients with hypertension. *J. Am. Coll. Cardiol.* **2007**, *49*, 1157–1163.

(8) Webb, R.; Schiering, N.; Sedrani, R.; Maibaum, J. Direct Renin Inhibitors as A New Therapy for Hypertension. *J. Med. Chem.* **2010**, *50*, 4832-4844.

(9) Tice, C. M. and Singh S. B. Evolution of Diverse Classes of Renin Inhibitors through the Years. In *Aspartic Acid Proteases as Therapeutic Targets*; Ghosh, A. K., Ed.; Methods and Principles in Medicinal Chemistry (Vol. 45), Mannhold, R.; Kubinyi, H.; Folkers, G., Eds.; Wiley-VCH: Weinheim, Germany, 2010, pp 297–324.

(10) (a) Maibaum, J.; Stutz, S.; Göschke, R.; Rigollier, P.; Yamaguchi, Y.; Cumin, F.; Rahuel, J.; Baum, H.-P.; Cohen, N.-C.; Schnell, C. R.; Fuhrer, W.; Grütter, M. G.; Schilling, W.; Wood, J. M. Structural modification of the P2' position of 2,7-dialkyl-substituted 5(*S*)-amino-4(*S*)-hydroxy-8-phenyl-octanecarboxamides: the discovery of aliskiren, a potent nonpeptide human renin inhibitor active after once daily dosing in marmosets. *J. Med. Chem.* **2007**, 50, 4832–4844. (b) Maibaum, J.; Feldman, D. L. Case history on Tekturna/Rasilez (aliskiren), a highly

efficacious direct oral renin inhibitor as a new therapy for hypertension. *Annu. Rev. Med. Chem.* **2009**, *44*, 105–127.

(11) Bursavich, M. G.; Rich, D. H. Designing non-peptide peptidomimetics in the 21st century: inhibitors targeting conformational ensembles. *J. Med. Chem.* **2002**, *45*, 541–558.

(12) (a) Märki, H. P.; Binggeli, A.; Bittner, B.; Bohner-Lang, V.; Breu, V.; Bur, D.; Coassolo, Ph.; Clozel, J. P.; D'Arcy, A.; Doebeli, H.; Fischli, W.; Funk, Ch.; Foricher, J.; Giller, T.; Grüninger, F.; Guenzi, A.; Güller, R.; Hartung, T.; Hirth, G.; Jenny, Ch.; Kansy, M.; Klinkhammer, U.; Lave, T.; Lohri, B.; Luft, F. C.; Mervaala, E. M. Müller, D. N.; Müller, M.; Montavon, F.; Oefner, Ch.; Qiu, C.; Reichel, A.; Sanwald-Ducray, P.; Scalone, M.; Schleimer, M.; Schmid, R.; Stadler, H.; Treiber, A.; Valdenaire, O.; Vieira, E.; Waldmeier, P.; Wiegand-Chou, R.; Wilhelm, M.; Wostl, W.; Zell, M.; Zell, R. Piperidine renin inhibitors: from leads to drug candidates. *Il Farmaco* **2001**, *56*, 21–27; and references cited therein. (b) Holsworth, D. D.; Cai, C.; Cheng, X.-M.; Cody, W. L.; Downing, D. M.; Erasga, N.; Lee, C.; Powell, N. A.; Edmunds, J. J.; Stier, M.; Jalaie, M.; Zhang, E.; McConnell, P.; Ryan, M. J.; Bryant, J.; Li, T.; Kasani, A.; Hall, E.; Subedi, R.; Rahim, M.; Maiti, S.. Ketopiperazine-based renin inhibitors: Optimization of the "C" ring. *Bioorg. Med. Chem. Lett.* **2006**, *16*(9), 2500-2504.

(13) Bezencon, O.; Bur, D.; Weller, T.; Richard-Bildstein, S.; Remeň, L.; Sifferlen, T.; Corminboeuf, O.; Grisostomi, C.; Boss, C.; Prade, L.; Delahye, S.; Treiber, A.; Strickner, P.; Binkert, C.; Hess, P.; Steiner, B.; Fischli, W. Design and preparation of potent, nonpeptidic, bioavailable renin inhibitors. *J. Med. Chem*. **2009**, *52*, 3689–3702.

(14) Jia, L.; Simpson, R. D.; Yuan, J.; Xu, Z.; Zhao, W.; Cacatian, S.; Tice, C. M.; Guo, J.; Ishchenko, A.; Singh, S. B.; Wu, Z; McKeever, B. M.; Bukhtiyarov, Y.; Johnson, Judith A.; Doe,

C. P.; Harrison, R. K.; McGeehan, G. M.; Dillard, L. W.; Baldwin, J. J. and Claremon D. A. Discovery of VTP-27999, an Alkyl Amine Renin Inhibitor with Potential for Clinical Utility. *ACS Med. Chem. Lett.* **2011**, 2, 747-751.

(15) Lorthiois E.; Breitenstein W.; Cumin F.; Ehrhardt C.; Francotte E.; Jacoby E.; Ostermann N.; Sellner H.; Takatoshi K.; Webb R.; Rigel D.; Hassiepen U.; Richert P.; Wagner T.; Maibaum J. The Discovery of Novel Potent *trans*-3,4-Disubstituted Pyrrolidine Inhibitors of the Human Aspartic Protease Renin from in silico Three-Dimensional (3D) Pharmacophore Searches. *J. Med. Chem*. submitted for publication.

(16) Ruedisser S.; Ehrhardt C.; Sedrani R.; Maibaum J. Unpublished results.

(17) Jones, G.; Willett, P.; Glen, R.C.; Leach, A.R.; Taylor, R. Development and Validation of a Genetic Algorithm for Flexible Docking. J. Mol. Biol., 1997, 267, 727-748.

(18) Tripos Inc., 1699 South Hanley Rd., St. Louis, Missouri, 63144, USA.

(19) See Supporting Information.

(20) Jacoby E.; Rüeger H.; Breitenstein W.; Marzinzik A. Unpublished results.

(21) The electron density map resolved to 2.6 Å resolution allowed the tentative assignment of the absolute configuration to be (3*S*,5*R*) for the single stereoisomer of **5** observed in the complex with rh-renin.[19] The pure enantiomers (3*S*,5*R*)-**5** and (3*R*,5*S*)-**5** were prepared from (3*S*,5*R*)-**11** and (3*R*,5*S*)-**11**, respectively. The eutomer (3*S*,5*R*)-**5** (IC_{50} = 0.5 μM) was at least 60-fold more potent toward rh-renin in the FRET biochemical assay than the distomer (3*R*,5*S*)-**5** (IC_{50} >30 μM). The absolute configuration for (3*S*,5*R*)-**5** was determined by small molecule X-ray diffraction.[19].

(22) For SAR exploration of peptide-like peptidomimetic renin inhibitors bearing polar S_1' residues, see: Atsuumi, S.; Nakano, M.; Koike, Y.; Tanaka, S.; Matsuyama, K.; Nakano, M.; Morishima, H. Renin inhibitors. I. Synthesis and structure-activity relationships of transition-state inhibitors containing homostatine analogs at the scissile bond. *Chem. Pharm. Bull.* **1992**, *40*, 364–370.

(23) Bissantz, C.; Kuhn, B.; Stahl, M. A medicinal chemist's guide to molecular interactions. J. *Med. Chem.* **2010**, *53*, 5061–5084.

(24) B Bohlender, J.; Fukamizu, A.; Lippoldt, A.; Nomura, T.; Dietz, R.; Menard, J.; Murakami, K.; Luft, F. C.; Ganten, D. High human hypertension in transgenic rats. *Hypertension* **1997**, *29*, 428–434.

Table of content Graphic